

Referee 1:

The authors have improved the manuscript considerably and many of the smaller issues with the previous version of the manuscript have been adequately addressed. However the recommended (by both reviewers) additional validation exercise of NO₂ using accurate ground-based observations has unfortunately not been carried out and I still think that this is a requirement for claiming an actual validation/verification of NO₂ rather than just a comparison of two uncertain datasets. This is particularly important given that MACC/CAMS is such a high-profile project, so the model performance for all species should be rigorously tested and documented.

As for the concern regarding the MNMB as an unusual validation metric, the authors provided a quite reasonable argument for it in the response to the reviewers but they did not expand/modify the description of the MNMB in the revised manuscript, which is where it actually matters. I still think that it is necessary to provide more detailed information about the statistical properties of the MNMB when it is introduced in the manuscript.

Referee 2:

The paper 'Evaluation of the MACC operational forecast system' has improved a lot since the last revision and I recommend it to be published subject to minor changes, mostly technical. There still remain some small questions, though, (points 13, 14, 25, 26, 27 below) that need to be answered:

1. Acronyms should be defined where they appear first, also in the abstract (e.g. SCIAMACHY, GOME, MOPITT, EU, MOZART, TM5, OASIS4, MLS, SBUV, OMI, IASI, MODIS, GEIA, FFED, GFAS, MEGAN, B3dCTM, FRESCO... I have certainly missed some, do a search for the first appearance).
2. page 3, line 2: replace 'and environment' with 'and the environment' (add a definite article).
3. page 3, line 4: remove the full stop and continue with lower case 'as'
4. page 3, line 10: replace 'and crop yields' with 'as well as crop yields'.
5. page 3, line 16: MACC has already been defined, delete the definition here.
6. page 3, line 18: CAMS also has been defined already, delete the definition.
7. page 5, lines 12 and 18: once you write 100 km x 100 km and another time 80 km, be consistent.
8. page 5, lines 13 and 19: once you write MOZART-3 another time MOZART version 3.5, be consistent.
9. page 5, line 24: replace 'out of the EU project' with 'from the EU project'.
10. page 7, line 18: it would be good to have an indication which stations provide CO and which O₃ in table 3

11. page 7, line 19: full stop after O₃ is in subscript.
12. page 7, line 20: replace 'the data in the database is' with 'the data in the database are'
13. page 7, line 29 and page 8, line 17: Motivate why for GAW 6 hourly model data are used and for EMEP 3 hourly model data and why the day night difference is only done for the EMEP data (e.g. 'We only used this data set to test the dependency of the biases on day and night data' or something like that).
14. page 8, line 1: What is the maximum altitude difference between the station and the model level, it would be good to know this.
15. page 9, line 8: replace 'In order for better data quality' with 'In order to achieve better data quality' or 'In order to get...' or something like this.
16. page 9, line 19: If with the sentence 'The model CO total columns used in the comparison with MOPITT observations, have been calculated using the averaging kernel smoothed profiles X* which have the same vertical resolution and a priori dependence as the MOPITT retrievals.' you mean 'The averaging kernel smoothed CO data X* have the same vertical resolution and a priori dependence as the MOPITT retrievals. These have been used to calculate averaging kernel smoothed model CO total columns which are compared to the MOPITT total columns.' then you should replace it. As it stands it is not clear.
17. page 10, line 17: 'Satellite observations are gridded to the horizontal model resolution'. Do you mean 'Satellite observations are interpolated to the resolution of the horizontal model grid.'
18. page 10, line 29: explain why Siberia and Alaska are excepted.
19. page 11, line 20: symbols are all superscripted they should be set down.
20. page 12, line 15: replace 'below' with 'bottom' (also in the Figure)
21. page 12, line 24: maybe better 'appears to be remedied' instead of 'has been' or put a reference for a validation for this.
22. page 13, line 32 and page 14, line 1: -9 is not a positive bias, please rephrase.
23. page 14, line 11: the 'larger' refers to larger negative and larger positive biases, please clarify.
24. page 14, line 29: Are the monthly MNMBs global? Please indicate if so.
25. page 28, line 28: I presume you don't use AK smoothed IASI data to compare with MOPITT data, as you did for the MACC comparisons. Depending on what you compare this discussion is not valid, since the AK smoothing should get rid of the a priori information (in the MACC-MOPITT comparison but might not in the IASI-MOPITT comparison). With the ingestion of the IASI CO into the model, the model

sees CO as IASI does. Depending on the shape of the IASI AK you might need to smooth the MOPITT data... Please check!

26. page 18, line 7: Is this likely because of more stations in the North?

27. page 18, line 9: Just looking at the data, could the biases not also come from a temperature dependency?

28. page 18, line 15: please replace 'the new model cycle and MOZART model version' with 'the new model cycle and the new MOZART model version'.

29. page 19, line 5: Please replace 'There is a close agreement' with 'There is close agreement'

30. page 19, line 9: Please replace 'are at a highest' with 'are highest'

31. page 21, line 6: Replace 'emissions.Inc nsistencies' with 'emissions. inconsistencies'.

32. page 21, line 8: Should there not be a 'forecast' or 'assimilation' after NRT?

Answers from the authors:

We have revised the paper concerning the following issues:

-As recommended, we have complemented our NO₂ validation exercise with ground-based observations. However, the observational data situation is more limited for NO₂ than for the other species. To ensure regional representativeness, we have put our focus only on stations in Europe.

-we have expanded the discussion regarding the use of the MNMB statistics

-we have addressed the points highlighted by referee 2.

Answers to referee 2:

1. Acronyms should be defined where they appear first, also in the abstract (e.g. SCIAMACHY, GOME, MOPITT, EU, MOZART, TM5, OASIS4, MLS, SBUV, OMI, IASI, MODIS, GEIA, FFED, GFAS, MEGAN, B3dCTM, FRESCO... I have certainly missed some, do a search for the first appearance

-done

2. page 3, line 2: replace 'and environment' with 'and the environment' (add a definite article).

-done

3. page 3, line 4: remove the full stop and continue with lower case 'as'

-done

4. page 3, line 10: replace 'and crop yields' with 'as well as crop yields'.

-done

5. page 3, line 16: MACC has already been defined, delete the definition here

-done

6. page 3, line 18: CAMS also has been defined already, delete the definition.

-done

7. page 5, lines 12 and 18: once you write 100 km x 100 km and another time 80 km, be consistent.

- 80 km is the resolution of the updated model cycle from July 2012 onwards

8. page 5, lines 13 and 19: once you write MOZART-3 another time MOZART version 3.5, be consistent.

-done

9. page 5, line 24: replace 'out of the EU project' with 'from the EU project'.

-done

10. page 7, line 18: it would be good to have an indication which stations provide CO and which O3 in table 3

-done

11. page 7, line 19: full stop after O3 is in subscript.

-done

12. page 7, line 20: replace 'the data in the database is' with 'the data in the database are'

-done

13. page 7, line 29 and page 8, line 17: Motivate why for GAW 6 hourly model data are used and for EMEP 3 hourly model data and why the day night difference is only done for the EMEP data (e.g. 'We only used this data set to test the dependency of the biases on day and night data' or something like that).

- done,

14. page 8, line 1: What is the maximum altitude difference between the station and the model level, it would be good to know this.

Altitude differences depend on model resolution, model orography and grid location. Over flat terrain altitude deviations between station and model level are <100m, mostly only few tens of m. Larger differences may occur for individual stations in complex terrain.

15. page 9, line 8: replace 'In order for better data quality' with 'In order to achieve better data quality' or 'In order to get...' or something like this.

-done

16. page 9, line 19: *If with the sentence 'The model CO total columns used in the comparison with MOPITT observations, have been calculated using the averaging kernel smoothed profiles X* which have the same vertical resolution and a priori dependence as the MOPITT retrievals.' you mean 'The averaging kernel smoothed CO data X* have the same vertical resolution and a priori dependence as the MOPITT retrievals. These have been used to calculate averaging kernel smoothed model CO total columns which are compared to the MOPITT total columns.'* then you should replace it. As it stands it is not clear.

-done

17. page 10, line 17: *'Satellite observations are gridded to the horizontal model resolution'. Do you mean 'Satellite observations are interpolated to the resolution of the horizontal model grid.'*

-The satellite data value for a specific model grid box is the average of all satellite NO₂ columns with a footprint falling into the model grid box. I.e., the data is not interpolated in space.

18. page 10, line 29: *explain why Siberia and Alaska are excepted.*

-Siberia and Alaska were excluded from the evaluation against SCIAMACHY/GOME-2, as the stratospheric correction method does not perform well at high latitudes, which can result in negative tropospheric NO₂ columns for these regions

19. page 11, line 20: *symbols are all superscripted they should be set down.*

-done

20. page 12, line 15: *replace 'below' with 'bottom' (also in the Figure)*

-done

21. page 12, line 24: *maybe better 'appears to be remedied' instead of 'has been' or put a reference for a validation for this.*

-done

22. page 13, line 32 and page 14, line 1: *-9 is not a positive bias, please rephrase.*

-done

23. page 14, line 11: *the 'larger' refers to larger negative and larger positive biases, please clarify.*

-done

24. page 14, line 29: *Are the monthly MNMBs global? Please indicate if so.*

-done

25. page 28, line 28: *I presume you don't use AK smoothed IASI data to compare with MOPITT data, as you did for the MACC comparisons. Depending on what you compare this discussion is not valid, since the AK smoothing should get rid of the a priori information (in the MACC-MOPITT comparison but might not in the IASI-MOPITT comparison). With the ingestion of the IASI CO into the model, the model sees CO as IASI does. Depending on the shape of the IASI AK you might need to smooth the MOPITT data... Please check!*

- This part of the paper refers to the George et al. (2009) paper, where the IASI CO columns are compared with the MOPITT CO columns adjusted with the IASI a priori (Rodgers and Connor (2003) or Luo et al. (2007)). On the global scale, the average difference was found to be less than 10%. In this paper, the MACC simulations are smoothed with the MOPITT averaging kernels. As the vertical resolutions of IASI and MOPITT are close, and the shapes of their averaging kernels are similar, it is acceptable to compare the MOPITT-AK smoothed MACC simulations with MOPITT on one hand and with IASI on the other hand.

26. page 18, line 7: *Is this likely because of more stations in the North?*

-yes, this statement is limited to the northern mid-latitudes. We have changed this in the text: “For stations located in the northern mid-latitudes, the evaluation between measured O₃ surface mixing ratios and the MACC_osuite reveals a seasonally dependent bias, with an underestimation of the observed O₃ mixing ratios during the winter season and an overestimation during the summer months. “

27. page 18, line 9: *Just looking at the data, could the biases not also come from a temperature dependency?*

Though temperature is indirectly affected by the photochemical ozone balance (via radiation) and stratification (nocturnal surface sink), there is no direct causal link between temperature and ozone concentrations in the model chemistry/physics.

28. page 18, line 15: *please replace 'the new model cycle and MOZART model version' with 'the new model cycle and the new MOZART model version'.*

-done

29. page 19, line 5: *Please replace 'There is a close agreement' with 'There is close agreement'*

-done

30. page 19, line 9: *Please replace 'are at a highest' with 'are highest'*

-done

31. page 21, line 6: *Replace 'emissions.Inc nsistencies' with 'emissions. inconsistencies.'*

-done

32. page 21, line 8: *Should there not be a 'forecast' or 'assimilation' after NRT?*

-done

1 **Evaluation of the MACC operational forecast system-**
2 **potential and challenges of global near-real-time modelling**
3 **with respect to reactive gases in the troposphere**

4

5

6 **A. Wagner¹, A.-M. Blechschmidt², I. Bouarar^{3[*]}, E.-G. Brunke⁴, C. Clerbaux³,**
7 **M. Cupeiro⁵, P. Cristofanelli⁶, H. Eskes⁷, J. Flemming⁸, H. Flentje¹, M.**
8 **George³, S. Gilge¹, A. Hilboll², A. Inness⁸, J. Kapsomenakis⁹, A. Richter², L.**
9 **Ries¹⁰, W. Spangl¹¹, O. Stein¹², R. Weller¹³, C. Zerefos⁹**

10 [1]{Deutscher Wetterdienst, Meteorologisches Observatorium Hohenpeissenberg, Germany}

11 [2]{Institute of Environmental Physics, University of Bremen, Germany}

12 [3]{Sorbonne Universités, UPMC Univ. Paris 06; Université Versailles St-Quentin;
13 CNRS/INSU, LATMOS-IPSL, Paris, France}

14 [4]{South African Weather Service, Stellenbosch, South Africa}

15 [5]{National Meteorological Service, Ushuaia, Tierra del Fuego, Argentina}

16 [6]{National Research Council of Italy, ISAC, Bologna, Italy}

17 [7]{Royal Netherlands Meteorological Institute, De Bilt, The Netherlands}

18 [8]{European Centre for Medium-range Weather Forecasts, Reading, UK}

19 [9]{Academy of Athens, Research Centre for Atmospheric Physics and Climatology, Athens,
20 Greece}

21 [10]{Federal Environment Agency, GAW Global Station Zugspitze/Hohenpeissenberg,
22 Zugspitze 5, D-82475 Zugspitze}

23 [11]{Umweltbundesamt GmbH, Air Pollution Control & Climate Change Mitigation, Vienna,
24 Austria}

25 [12]{Forschungszentrum Jülich, IEK-8 (Troposphere), Jülich, Germany}

26 [13]{Alfred Wegener Institute, Bremerhaven, Germany}

27

1 [*]{now at: Max-Planck-Institut for Meteorology, Hamburg, Germany}

2 Correspondence to: A. Wagner (Annette.wagner@dwd.de)

3

4 **Abstract**

5 Monitoring Atmospheric Composition and Climate (MACC) represented the European
6 Union's Copernicus Atmosphere Monitoring Service (CAMS) (<http://www.copernicus.eu/>),
7 which became fully operational in the course of 2015. The global near-real-time MACC
8 model production run for aerosol and reactive gases provides daily analyses and 5-day
9 forecasts of atmospheric composition fields. It is the only assimilation system world-wide that
10 is operational to produce global analyses and forecasts of reactive gases and aerosol fields.
11 We have investigated the ability of the MACC analysis system to simulate tropospheric
12 concentrations of reactive gases (CO, O₃, and NO₂) covering the period between 2009 and
13 2012. A validation was performed based on CO, NO₂ and O₃ surface observations from the
14 Global Atmosphere Watch (GAW) network, O₃ surface observations from the European
15 Monitoring and Evaluation Programme (EMEP) and furthermore, NO₂ tropospheric columns,
16 as well as CO total columns derived from satellite sensors. The MACC system proved
17 capable of reproducing reactive gas concentrations in consistent quality, however, with a
18 seasonally dependent bias compared to surface and satellite observations: For northern
19 hemisphere surface O₃ mixing ratios, positive biases appear during the warm seasons and
20 negative biases during the cold parts of the years, with monthly Modified Normalised Mean
21 Biases (MNMBs) ranging between -30% and 30% at the surface. Model biases are likely to
22 result from difficulties in the simulation of vertical mixing at night and deficiencies in the
23 model's dry deposition parameterization. Observed tropospheric columns of NO₂ and CO
24 could be reproduced correctly during the warm seasons, but are mostly underestimated by the
25 model during the cold seasons, when anthropogenic emissions are at a highest, especially over
26 the US, Europe and Asia. Monthly MNMBs of the satellite data evaluation range between
27 -110% and 40% for NO₂ and at most -20% for CO, over the investigated regions. The
28 underestimation is likely to result from a combination of errors concerning the dry deposition
29 parameterization and certain limitations in the current emission inventories, together with an
30 insufficiently established seasonality in the emissions.

Gelöscht: currently

Gelöscht: s

Gelöscht: will become

Gelöscht: the course of

Formatiert: Tiefgestellt

Gelöscht: the

Gelöscht: SCIAMACHY and GOME-2, and CO total columns derived from the satellite sensor MOPITT.

1 Introduction

The impact of reactive gases on climate, human health and the environment has gained increasing public and scientific interest in the last decade (Bell et al., 2006; Cape 2008; Mohnen et al., 2013; Seinfeld and Pandis 2006; Selin et al., 2009) as air pollutants such as carbon monoxide (CO), nitrogen oxides (NO_x) and ozone (O₃) are known to have acute and chronic effects on human health, ranging from minor upper respiratory irritation to chronic respiratory and heart disease, lung cancer, acute respiratory infections in children and chronic bronchitis in adults (Bell et al., 2006; Kampa and Castanas 2006). Tropospheric ozone, even in small concentrations, is also known to cause plant damage in reducing plant primary productivity as well as crop yields (e.g. Ashmore 2005). It is also contributing to global warming by direct and indirect radiative forcing (Forster et al., 2007, Sitch et al., 2007). Pollution events can be caused by local sources and processes but are also influenced by continental and intercontinental transport of air masses. Global models can provide the transport patterns of air masses and deliver the boundary conditions for regional models, facilitating the forecast and investigation of air pollutants.

Gelöscht: As

Gelöscht: and

The European Union (EU)-funded research project MACC (consisting of a series of European projects, MACC to MACC-III), provides the preparatory work that will form the basis of the Copernicus Atmosphere Monitoring Service. This service is established by the EU to provide a range of products of societal and environmental value with the aim to help European governments respond to climate change and air quality problems. MACC provides reanalysis, monitoring products of atmospheric key constituents (e.g. Inness et al., 2013), as well as operational daily forecasting of greenhouse gases, aerosols and reactive gases (Benedetti et al., 2011; Stein et al., 2012) on a global and on European-scale level, and derived products such as solar radiation. An important aim of the MACC system is to describe the occurrence, magnitude and transport pathways of disruptive events, e.g., volcanoes (Flemming and Inness, 2013), major fires (Huijnen et al., 2012; Kaiser et al., 2012) and dust storms (Cuevas et al., 2015). The product catalogue can be found on the MACC website, <http://copernicus-atmosphere.eu>. For the generation of atmospheric products, state-of-the-art atmospheric modelling is combined with assimilated satellite data (Hollingsworth et al., 2008, Inness et al., 2013, 2015, more general information about data assimilation can be found in e.g. Ballabrera-Poy et al., 2009 or Kalnay 2003). Within the MACC project there is a dedicated validation

Gelöscht: - Monitoring Atmospheric Composition and Climate,

Gelöscht: (CAMS)

1 activity to provide up-to-date information on the quality of the reanalysis, daily analyses and
2 forecasts. Validation reports are updated regularly and are available on the MACC websites.

3 The MACC global near-real-time (NRT) production model for reactive gases and aerosol has
4 operated with data assimilation from September 2009 onwards, providing boundary
5 conditions for the MACC regional air quality products (RAQ), and other downstream users.

6 The model simulations also provide input for the stratospheric ozone analyses delivered in
7 near-real-time by the MACC stratospheric ozone system (Lefever et al., 2014).

8 In this paper we describe the investigation of the potential and challenges of near-real-time
9 modelling with the MACC analysis system between 2009 and 2012. We concentrate on this
10 period because of the availability of validated independent observations, namely surface
11 observations from the Global Atmosphere Watch Programme GAW, the European
12 Monitoring and Evaluation Programme EMEP, as well as total column/tropospheric column
13 satellite data from the MOPITT (Measurement Of Pollution In The Troposphere),
14 SCIAMACHY (SCanning Imaging Absorption spectroMeter for Atmospheric CHartography)
15 and GOME-2 (Global Ozone Monitoring Experiment-2) sensors, that are used for comparison.

16 In particular, we study the model's ability to reproduce the seasonality and absolute values of
17 CO and NO₂ in the troposphere as well as NO₂, O₃ and CO at the surface. The impact of
18 changes in model version, data assimilation and emission inventories on the model
19 performance is examined and discussed. The paper is structured in the following way: Section
20 2 contains a description of the model and the validation data sets as well as the applied
21 validation metrics. Section 3 presents the validation results for CO, NO₂ and O₃. Section 4
22 provides the discussion and section 5 the conclusions of the paper.

23 **2 Data and methods**

24 **2.1 The MACC model system in the 2009-2012 period**

25 The MACC global products for reactive gases consist of a reanalysis performed for the years
26 2003-2012 (Inness et al., 2013) and the near-real-time analysis and forecast, largely based on
27 the same assimilation and forecasting system, but targeting different user groups. The Model
28 for OZone And Related chemical Tracers (MOZART) chemical transport model (CTM) is
29 coupled to the Integrated Forecast System (IFS) of the European Centre for Medium-Range
30 Weather forecast (ECMWF), which together represent the MOZART-IFS model system
31 (Flemming et al., 2009 and Stein et al. 2012). An alternative analysis system has been set up

Gelöscht: (

Gelöscht:

Gelöscht:)

Formatiert: Tiefgestellt

Gelöscht:

Gelöscht: Methods

1 | based on the global [chemistry Transport Model version 5 \(TM5, see also Huijnen et al.,](#)
2 | 2010). Details of the MOZART version used in the MACC global products can be found in
3 | Kinnison et al., 2007 and Stein et al. (2011, 2012). In the simulation, the IFS and the
4 | MOZART model run in parallel and exchange several two- and three-dimensional fields
5 | every model hour using the [Ocean Atmosphere Sea Ice Soil version 4 \(OASIS4\)](#) coupling
6 | software (Valcke and Redler 2006), thereby producing three-dimensional IFS fields for O₃,
7 | CO, SO₂, NO_x, HCHO, sea salt aerosol, desert dust, black carbon, organic matter, and total
8 | aerosol. The IFS provides meteorological data to MOZART. Data assimilation and transport
9 | of the MACC species takes place in IFS, while the whole chemical reaction system is
10 | calculated in MOZART.

Gelöscht: CTM

Gelöscht: (

11 | The MACC_osuite (operational suite) is the global near-real-time MACC model production
12 | run for aerosol and reactive gases. Here, we have investigated only the MACC analysis. In
13 | contrast to the reanalysis, the MACC_osuite is a near-real-time run, which implies that it is
14 | only run once in near-real-time and may thus contain inconsistencies in e.g. the assimilated
15 | data. The MACC_osuite was based on the IFS cycle CY36R1 with IFS model resolution of
16 | approximately 100 km by 100 km at 60 levels (T159L60) from September 2009 until July
17 | 2012. The gas-phase chemistry module in this cycle is based on MOZART, [version 3.0](#)
18 | (Kinnison et al., 2007). The model has been upgraded, following updates of the ECMWF
19 | meteorological model and MACC-specific updates, i.e. in chemical data assimilation and with
20 | respect to the chemical model itself. Thus, from July 2012 onwards, the MACC_osuite has
21 | run with a change of the meteorological model to a new IFS cycle (version CY37R3), with an
22 | IFS model resolution of approximately 80 km at 60 levels (T255L60) and an upgrade of the
23 | MOZART version 3.5 (Kinnison et al., 2007; Emmons et al., 2011; Stein et al. 2013). This
24 | includes, amongst others, updated velocity fields for the dry deposition of O₃ over ice, as
25 | described in Stein et al. (2013). A detailed documentation of system changes can be found at:
26 | http://www.copernicus-atmosphere.eu/oper_info/nrt_info_for_users/

Gelöscht: -3

27 | 2.1.1 Emission inventories and assimilated data sets

28 | In the MACC_osuite, anthropogenic emissions are based on emissions [from](#) the EU project
29 | [REanalysis of the TRopospheric chemical composition Over the past 40 years \(RETRO\)](#) merged
30 | with updated emissions for East Asia from the [Regional Emission inventory in ASia \(REAS\)](#)
31 | inventory, (Schultz et al. 2007) in the following referred to as RETRO-REAS. The horizontal

Gelöscht: out of

Formatiert: Englisch
(Großbritannien)

Formatiert: Schriftart: Nicht
Kursiv, Englisch (Großbritannien)

Formatiert: Englisch
(Großbritannien)

Formatiert: Englisch
(Großbritannien)

1 resolution is 0.5° in latitude and longitude and it contains a monthly temporal resolution.
2 Biogenic emissions are taken from [Global Emissions Initiative \(GEIA\)](#), fire emissions are
3 based on a climatology derived from [Global Fire Emissions Database version 2 \(GFEDv2,](#)
4 [van der Werf et al., 2006\)](#) until April 2010, when fire emissions change to [Global Fire](#)
5 [Assimilation System \(GFAS\)](#) emissions (Kaiser et al., 2012). Between January 2011 and
6 October 2011 there has been a fire emission reading error in the model, where, instead of
7 adjusting emissions to the appropriate month, the same set of emissions have been read
8 throughout this period.

Gelöscht: (

Gelöscht: fire

9 After the model upgrade to the new cycle version CY37R3, in July 2012, the emission
10 inventories changed from the merged RETRO-REAS and GEIA inventories, used in the
11 previous cycle, to the MACCcity anthropogenic and biogenic emissions (Granier et al., 2011)
12 and (climatological) [Model of Emissions of Gases and Aerosols from Nature version 2](#)
13 [\(MEGAN-v2, see Guenther et al., 2006\)](#) emission inventories. Wintertime anthropogenic CO
14 emissions are scaled up over Europe and North America (see Stein et al., 2014). Near-real-
15 time fire emissions are taken from GFASv1.0 (Kaiser et al. 2012), for both gas-phase and
16 aerosol.

Formatiert: Englisch
(Großbritannien)

Formatiert: Schriftart: Nicht
Kursiv, Englisch (Großbritannien)

Formatiert: Englisch
(Großbritannien)

Gelöscht: (

17 In the MACC_suite, the initial conditions for some of the chemical species are provided by
18 data assimilation of atmospheric composition observations from satellites (see Benedetti et
19 al., 2009, Inness et al., 2009, 2013, Massart et al., 2014). Table 1 lists the assimilated data
20 products. From September 2009 to June 2012, O₃ total columns of the [Microwave Limb](#)
21 [Sounder \(MLS\)](#) and [Solar Backscatter Ultraviolet \(SBUV-2\)](#) instruments are assimilated, as
22 well as [Ozone Monitoring Instrument \(OMI\)](#) and SCIAMACHY total columns (the latter only
23 until March 2012, when the European Space Agency lost contact with the ENVironmental
24 SATellite ENVISAT). CO total columns are assimilated from the [Infrared Atmospheric](#)
25 [Sounding Interferometer \(IASI\)](#) sensor and aerosol total optical depth is assimilated from the
26 [Moderate Resolution Imaging Spectroradiometer \(MODIS\)](#) instrument. After the model cycle
27 update in July 2012, data assimilation also contains OMI tropospheric columns of NO₂ and
28 SO₂, as well as CO MOPITT total columns. The CO total columns retrieved by MOPITT and
29 IASI instruments have a relatively similar seasonality, but there is a systematic difference
30 with MOPITT CO being higher over most regions in the northern hemisphere, especially
31 during winter and spring. George et al. (2015) investigated the differences between MOPITT
32 and IASI, and showed the impact of a priori information on the retrieved measurements.

Gelöscht: ;

Gelöscht: ;

Formatiert: Englisch
(Großbritannien)

Formatiert: Englisch
(Großbritannien)

Gelöscht: "An examination of the
long-term CO records from
MOPITT and IASI and comparison
of retrieval methodology", AMTD,
2015 submitted)

1 Table 1 and 2 summarize the data assimilation and setup of the MACC_osuite.

2 2.2 Validation data and methodology

3 In this study, mainly the same evaluation data sets have been used as during the MACC near-
4 real-time validation exercise. This implies some discontinuities in the evaluations, e.g. the
5 substitution of SCIAMACHY data with GOME-2 data after the loss of the ENVISAT sensor
6 or an exclusion of MOPITT satellite data after the start of its assimilation into the model. The
7 continuous process of updating and complementation of data sets in databases requires the
8 selection and definition of an evaluation data set at some point. The comparatively small
9 inconsistencies between our data sets are considered to have a negligible impact on the overall
10 evaluation results.

11 2.2.1 GAW surface O₃, CO and NO₂ observations

12 The Global Atmosphere Watch (GAW) programme of the World Meteorological
13 Organization (WMO) has been established to provide reliable long-term observations of the
14 chemical composition and physical properties of the atmosphere, which are relevant for
15 understanding atmospheric chemistry and climate change (WMO, 2013). GAW tropospheric
16 O₃ measurements are performed in a way to be suitable for the detection of long-term regional
17 and global changes. Furthermore, the GAW measurement programme focuses on
18 observations, which are regionally representative and should be free from influence of
19 significant local pollution sources and suited for the validation of global chemistry climate
20 models (WMO 2007). Detailed information on GAW and GAW related O₃, CO and NO₂
21 measurements can be found in WMO (2010, 2011 and 2013).

22 Hourly O₃, CO and NO₂ data have been downloaded from the WMO/GAW World Data Centre
23 for Greenhouse Gases (WDCGG) for the period between 09/2009 and 12/2012 (status of
24 download: 07/2013). Our evaluation includes 6 stations with surface observations for NO₂, 29
25 stations for CO and 50 stations with surface observations for O₃. Table 3 lists the geographic
26 coordinates and altitudes of the individual stations. Being a long-term data network, the data
27 in the database are provided with a temporal delay of approximately 2 years. As the data in
28 the database become sparse towards the end of the validation period, near-real-time
29 observations, as used in the MACC-project for near-real-time validation, presented on the
30 MACC website, have been included to complement the validation data sets. For the detection
31 of long-term trends and year-to-year variability, the data quality objectives (DQOs) for CO in

Gelöscht: Surface

Formatiert: Tiefgestellt

Gelöscht: CO O

Gelöscht:

Formatiert: Tiefgestellt

Gelöscht: CO

Gelöscht:

Gelöscht: CO

Formatiert: Tiefgestellt

Gelöscht: with surface observations

Formatiert: Nicht Hochgestellt/Tiefgestellt

Gelöscht: is

Gelöscht: s

1 GAW measurements are set to a maximum uncertainty of ± 2 ppb and to ± 5 ppb for marine
2 boundary layer sites and continental sites that are influenced by regional pollution and to ± 1
3 ppb for ozone (WMO, 2012, 2013) and 0.08 ppb for NO₂ (WMO 2011).

Formatiert: Tiefgestellt

Formatiert: Nicht Hochgestellt/
Tiefgestellt

4 For the evaluation with GAW station data, 6-hourly values (0, 6, 12, 18 UTC) of the analysis
5 mode have been extracted from the model and are matched with hourly observational GAW
6 station data. Model mixing ratios at the stations' location have been linearly interpolated from
7 the model data in the horizontal. In the vertical, modelled gas mixing ratios have been
8 extracted at the model level, which is closest to the GAW stations' altitude. Validation scores
9 (see section 2.3) have been calculated for each station between the 6-hourly model analysis
10 data and the corresponding observational data for the entire period (09/2009- 12/2012) and as
11 monthly averages.

Gelöscht: Surface

Gelöscht: Observations

12 2.2.2 EMEP surface O₃ observations

13 The European Monitoring and Evaluation Programme (EMEP) is a scientifically based and
14 policy driven programme under the Convention on Long-Range Transboundary Air Pollution
15 (CLRTAP) for international co-operation to solve transboundary air pollution problems.
16 Measurements of air quality in Europe have been carried out under the EMEP since 1977.

17 A detailed description of the EMEP measurement programme can be found in Tørseth et al.
18 (2012). The surface hourly ozone data between 09/2009 and 12/2012 have been downloaded
19 from the EMEP data web-page (<http://www.nilu.no/projects/ccc/emepdata.html>). For the
20 validation, only stations meeting the 75% availability threshold per day and per month are
21 taken into account. The precision is close to 1.5 ppb for a 10s measurement. More
22 information about the ozone data quality, calibration and maintenance procedures can be
23 found in Aas et al. (2000).

24 For comparison with EMEP data, 3-hourly model values (0, 3, 6, 12, 15, 18, 21 UTC) of the
25 analysis mode have been chosen. We used this data set to test the dependency of the biases on
26 day and night time basis, separately. Gas mixing ratios have been extracted from the model
27 and are matched with hourly observational surface ozone data at 124 EMEP stations in the
28 same way as for the GAW station data. The EMEP surface ozone values and the interpolated
29 surface modeled values are compared on a monthly basis for the latitude bands of 30°N –
30 40°N (southern Europe), 40°N – 50°N (central Europe) and 50°N – 70°N (northern Europe).
31 For the identification of differences in the MACC_osuite performance between day and night
32 time, the MACC_osuite simulations and the EMEP observations for the three latitude bands

Formatiert: Schriftartfarbe:
Automatisch

Gelöscht: , in order to be able to
evaluate day and night time
performance of the model

1 have been additionally separated into day-time (12:00–15:00 Local Time LT) and night-time
2 (00:00–03:00 LT) intervals.

3 **2.2.3 MOPITT CO total column retrievals**

4 The MOPITT (Measurement Of Pollution In The Troposphere) instrument is mounted on
5 board the NASA EOS Terra satellite and provides CO distributions at the global scale (Deeter
6 et al., 2004). MOPITT has a horizontal resolution of 22 km x 22 km and allows global
7 coverage within 3 days. The data used in this study corresponds to CO total columns from
8 version 5 (V5) of the MOPITT thermal infrared (TIR) product level 3. This product is
9 available via the following web server: <http://www2.acd.ucar.edu/mopitt/products>. Validation
10 of the MOPITT V5 product against in-situ CO observations showed a mean bias of 0.06×10^{18}
11 molecules cm^{-2} (Deeter et al., 2013). Following the recommendation in the users' guide,
12 (www.acd.ucar.edu/mopitt/v5_users_guide_beta.pdf), the MOPITT data were averaged by
13 taking into account their relative errors provided by the Observation Quality Index (OQI).

14 Also, in order to achieve better data quality we used only daytime CO data since retrieval
15 sensitivity is greater for daytime rather than nighttime overpasses. A further description of the
16 V5 data is presented in Deeter et al. (2013) and Worden et al. (2014).

17 For the validation, the model CO profiles (X) were transformed by applying the MOPITT
18 averaging kernels (A) and the a priori CO profile (X_a) according to the following equation
19 (Rodgers, 2000) to derive the smoothed profiles X^* appropriate for comparison with
20 MOPITT data:

$$21 \quad X^* = X_a + A(X - X_a)$$

22 Details on the method of calculation are referred to in Deeter et al. (2004) and Rodgers
23 (2000). The averaging kernels indicate the sensitivity of the MOPITT measurement and
24 retrieval system to the true CO profile, with the remainder of the information set by the a
25 priori profile and retrieval constraints (Emmons, 2009; Deeter et al., 2010). The CO data X^*
26 (derived using the above equation) have the same vertical resolution and a priori dependence
27 as the MOPITT retrievals and have been used to calculate averaging kernel smoothed model
28 CO total columns, which are compared to the MOPITT CO total columns. For the evaluation,
29 8 regions are defined (see Fig. 1): Europe, Alaska, Siberia, North Africa, South Africa, South
30 Asia, East Asia and the United States.

Gelöscht: for

Formatiert: Englisch (USA)

Formatiert: Englisch (USA)

Formatiert: Englisch (USA)

Formatiert: Englisch (USA)

Formatiert: Englisch (USA)

Gelöscht: The model CO total columns used in the comparison with MOPITT observations, have been calculated using the averaging kernel smoothed profiles X^* which have the same vertical resolution and a priori dependence as the MOPITT retrievals.

1 The model update in July 2012 includes an integration of MOPITT CO total columns in the
2 model's data assimilation system. With this, the MOPITT validation data has lost its
3 independency for the rest of the validation period and MOPITT validation data has thus only
4 been used until June 2012 for validation purposes.

5 **2.2.4 SCIAMACHY and GOME-2 NO₂ satellite observations**

Gelöscht: Satellite

Gelöscht: Observations

6 The SCanning Imaging Absorption spectrometer for Atmospheric CHartography
7 (SCIAMACHY; Bovensmann et al., 1999) onboard the ENVISAT and the Global Ozone
8 Monitoring Experiment-2 (GOME-2; Callies et al., 2000) onboard the Meteorological
9 Operational Satellite-A (MetOp-A) comprise UV-VIS and NIR sensors designed to provide
10 global observations of atmospheric trace gases.

11 In this study, the tropospheric NO₂ column data set described in Hilboll et al. (2013a) has
12 been used. In short, the measured radiances are analysed using Differential Optical
13 Absorption Spectroscopy (DOAS), (Platt and Stutz, 2008) in the 425–450 nm wavelength
14 window (Richter and Burrows, 2002). The influence of stratospheric NO₂ air masses has been
15 accounted for using the algorithm detailed by Hilboll et al. (2013b), using stratospheric NO₂
16 fields from the Bremen 3D Chemistry and Transport Model (B3dCTM, see also, Sinnhuber et
17 al., 2003a; Sinnhuber et al., 2003b; Winkler et al., 2008). Tropospheric air mass factors have
18 been calculated with the radiative transfer model SCIATRAN (Rozanov et al., 2005). Only
19 measurements with Fast RETrieval Scheme for Cloud from Oxygen A band (FRESCO+)
20 algorithm (Wang et al., 2008) cloud fractions of less than 20% are used.

Gelöscht: model (

Formatiert: Englisch
(Großbritannien)

Formatiert: Englisch
(Großbritannien)

21 Tropospheric NO₂ vertical column density (VCD) from the MACC_osuite is compared to
22 tropospheric NO₂ VCD from GOME-2 and SCIAMACHY. As the European Space Agency
23 lost contact with ENVISAT in April 2012, GOME-2 data is used for model validation from 1
24 April 2012 onwards, while SCIAMACHY data is used for the remaining time period
25 (September 2009 to March 2012). Satellite observations are gridded to the horizontal model
26 resolution, i.e. 1.875° for IFS cycle CY36R1 (09/2009 -06/2012) and 1.125° for cycle
27 CY37R3 (07/2012- 12/2012).

28 A few processing steps are applied to the MACC_osuite data to account for differences to the
29 satellite data such as observation time. Firstly, model data are vertically integrated to
30 tropospheric NO₂ VCDs by applying National Centers for Environmental Prediction (NCEP)
31 reanalysis (Kalnay et al., 1996) climatological tropopause pressure shown in Fig.1 of Santer et

1 al. (2003). Secondly, simulations are interpolated linearly in time to the SCIAMACHY
2 equator crossing time (roughly 10:00 LT). This most likely leads to some minor
3 overestimation of model NO₂ VCDs compared to GOME-2 data, as the equator crossing time
4 for GOME-2 is about 9:30 LT. Moreover, only model data for which corresponding satellite
5 observations exist are considered. For the evaluation, the same regions have been used as for
6 MOPITT (Fig.1), except for Siberia and Alaska. In contrast to MOPITT data, no averaging
7 kernel is applied.

8 Satellite observations of tropospheric NO₂ columns have relatively large uncertainties, mainly
9 linked to incomplete stratospheric correction (important over clean regions and at high
10 latitudes in winter and spring) and to uncertainties in air mass factors (mainly over polluted
11 regions) (e.g. Boersma et al., 2004 and Richter et al., 2005). The uncertainty varies with
12 geolocation and time but in first approximation can be separated into an absolute error of
13 5×10^{14} molec cm⁻² and a relative error of about 30%, whichever is larger. As some of the
14 contributions to this uncertainty are systematic, averaging over longer time periods does not
15 reduce the errors as much as one would expect for random errors. Over polluted regions, the
16 uncertainty from random noise in the spectra is small in comparison to other error sources, in
17 particular for monthly averages.

18 **2.3 Validation metrics**

19 A comprehensive model evaluation requires the selection of validation metrics that provide
20 complementary aspects of model performance. The following metrics have been used in the
21 evaluation:

22 **Modified Normalized Mean Bias MNMB**

$$23 \quad MNMB = \frac{2}{N} \sum_i \frac{f_i - o_i}{f_i + o_i} \quad (1)$$

24 **Root Mean Square Error RMSE**

$$25 \quad RMSE = \sqrt{\frac{1}{N} \sum_i (f_i - o_i)^2} \quad (2)$$

26 **Correlation Coefficient**

1 underestimation compensating each other, can lead to a small MNMB for the overall period.
2 For this reason, it is important to additionally consider an absolute measure, such as the
3 RMSE. However, it has to be noted that the RMSE is strongly influenced by larger values and
4 outliers, due to squaring. The correlation coefficient R can vary between 1 (perfect
5 correlation) and -1 (negative correlation) and is an important measure to check the linearity
6 between model and observations.

7 3 Results

8 3.1 Evaluation of ozone

9 The evaluation of the MACC_osuite run with O₃ from GAW surface observations (described
10 in section 2.2.1) demonstrates good agreement in absolute values and seasonality for most
11 regions. Figure 2 shows maps with Modified Normalized Mean Bias (MNMB, see section
12 2.3) evaluations for 50 GAW stations globally (top) and in Europe (bottom). Figure 3 presents
13 selected time series plots representing the results for high latitudes, low latitudes and Europe.
14 Large negative MNMBs over the whole period 09/2009 to 12/2012 (-30 to -82%) are
15 observed for stations located in Antarctica (Neumayer-NEU, South Pole-SPO, Syowa-SYO
16 and Concordia- CON) whereby O₃ surface mixing ratios are strongly underestimated by the
17 model. For stations located in high latitudes in the northern hemisphere (Barrow-BAR, Alaska
18 and Summit-SUM, Denmark), the MACC_osuite exhibits similar underestimated values of up
19 to -35% for the whole evaluation period. The time series plots for Arctic and Antarctic
20 stations (e.g. Summit-SUM, Neumayer-NEU and South Pole-SPO) in Fig. 3 show that an
21 underestimation visible in these regions appears to be remedied and model performance
22 improved with an updated dry deposition parameterization over ice, which has been
23 introduced with the new model cycle in July 2012 (see section 2.1).

24 Large positive MNMBs (up to 50 to 70%, Fig. 2) are observed for stations that are located in
25 or nearby cities and thus exposed to regional sources of contamination (Iskrba-ISK Slovenia,
26 Tsukuba- TSU, Japan, Cairo-CAI, Egypt). In tropical and subtropical regions, O₃ surface
27 mixing ratios are systematically overestimated (by about 20% on average) during the
28 evaluation period. The time series plots for tropical and subtropical stations (e.g. for Ragged
29 Point-RAG, Barbados and Cape Verde Observatory, Cape Verde –CVO, Fig. 3) reveal a
30 slight systematic positive offset throughout the year, however with high correlation
31 coefficients (0.6 on average).

Gelöscht: Ozone

Gelöscht: below

Gelöscht: has been

1 For GAW stations in Europe, the evaluation of the MACC_osuite for the whole period shows
2 MNMBs between -80 and 67%. Large biases appear only for 2 GAW stations located in
3 Europe: Rigi- RIG, Switzerland (-80%), located near mountainous terrain and Iskrba- ISK,
4 Slovenia (67%). For the rest of the stations MNMBs lie between 22 and -30%. Root Mean
5 Square Errors (RMSEs, see section 2.3) range between 7 and 35 ppb (15 ppb on average).
6 Again, results for Iskrba-ISK and Rigi-RIG show the largest errors. All other stations show
7 RMSEs between 7 and 20 ppb. Correlation coefficients here range between 0.1 and 0.7 (with
8 0.5 on average). Table 4 summarizes the results for all stations individually.

9 Monthly MNMBs (see Fig. 4) show a seasonally varying bias, with positive MNMBs
10 occurring during the northern summer months (with global average ranging between 5 and
11 29% during the months June and October), and negative MNMBs during the northern winter
12 months (between -2 and -33% during the months December to March). These deviations
13 partly cancel each other out in MNMB for the whole evaluation period. For the RMSEs, (Fig.
14 5) maximum values also occur during the northern summer months with global average
15 ranging between 11 and 16 ppb for June to September. The smallest errors appear during the
16 northern hemisphere winter months (global average falling between 8 and 10 ppb for
17 December and January). The correlation does not show a distinct seasonal behaviour (see Fig.
18 6).

19 The time series plots in Fig. 3 show that the seasonal cycle of O₃ mixing ratios with maximum
20 concentrations during the summer months and minimum values occurring during winter times
21 for European stations (e.g. Monte Cimone-MCI, Italy, Kosetice-KOS, Czech Republic, and
22 Kovk- KOV, Slovenia), could well be reproduced by the model, although there is some
23 overestimation in summer resulting mostly from observed minimum concentrations that are
24 not captured correctly by the MACC_osuite, (Kosetice-KOS, Czech Republic, and Kovk-
25 KOV, Slovenia).

26 The validation with EMEP surface ozone observations (described in section 2.2.2) in three
27 different regions in Europe for the period 09/2009 to 12/2012 likewise confirms the behaviour
28 of the model to overestimate O₃ mixing ratios during the warm period and underestimate O₃
29 concentrations during the cold period of the year (see Fig. 7). The mostly positive bias (May-
30 November) is between -9 and 56% for northern Europe and Central Europe and between 8%
31 and 48% for Southern Europe. Negative MNMBs appear, in accordance with GAW validation
32 results, during the winter-spring period (December-April) ranging between -48 and -7% for

1 EMEP stations in northern Europe (exception: December 2012 with 25%), between -1
2 and -39% in central Europe (exception: December 2012 with 31%), whereas in southern
3 Europe, deviations are smaller and remain mostly positive (between -8 and 9%) in winter
4 (exception: December 2012 with 37%). The different behaviour for December 2012 likely
5 results from the limited availability of observations towards the end of the validation period.
6 The separate evaluation of day and night-time O₃ mixing ratios (Fig. 8) shows that for
7 northern Europe night time biases exceed day time biases during all seasons. For central
8 Europe and southern Europe night-time biases are larger (negative MNMBs) during cold
9 periods (December–April), whereas during warm periods (May–November) larger biases
10 (positive MNMBs) appear during day time.

Gelöscht: larger biases appear during night time.

11 3.2 Evaluation of carbon monoxide

Gelöscht: Carbon

Gelöscht: Monoxide

12 The evaluation of the MACC_osuite with surface observations of 29 GAW stations (described
13 in section 2.2.1) shows that over the whole period September 2009 to December 2012, CO
14 mixing ratios could be reproduced with an average MNMB of -10%. The MNMBs for all
15 stations range between -50 and +30%. Results are listed in Table 5, a selection of time series
16 plots shows the results for stations in Europe, Asia and Canada in Fig. 9. MNMBs exceeding
17 $\pm 30\%$ appear for stations that are either located in or nearby cities and thus exposed to
18 regional sources of contamination (Kosetice- KOS, Czech Republic) or are located in or near
19 complex mountainous terrain (Rigi-RIG, Switzerland, BEO Moussala- BEO, Bulgaria) which
20 is not resolved by the topography of the global model. RMSEs fall between 12 and 143 ppb
21 (on average 48 ppb) for all stations during the validation period, but for only four stations
22 (Rigi-RIG, Kosetice- KOS, Payerne-PAY, Switzerland and BEO Moussala-BEO, all located
23 in Europe) do the RMSEs exceed 70 ppb. Correlation coefficients from the comparison with
24 GAW station data calculated over the whole time period range between 0 and 0.8 (on average
25 0.4), with only four stations showing values smaller than 0.2 (Rigi-RIG, Moussala-BEO, East
26 Trout Lake-ETL and Lac la Biche-LAC (the latter two located in Canada).

27 Considering the global monthly MNMBs and RMSEs, it can be seen that during the northern
28 hemisphere summer months, June to September, both are small (absolute differences less than
29 5%), see Fig. 10 and Fig. 11. Negative MNMBs (up to -35%) and larger RMSEs (up to 72
30 ppb) appear during the northern hemisphere winter months, November to March, when
31 anthropogenic emissions are at a highest, especially for the US, northern latitudes and Europe.
32 Monthly correlation coefficients are between 0.1 and 0.5 and do not show a distinct seasonal

1 behaviour (see Fig. 12), the low values of 0.1 during the period January 2011 to October 2011
2 result from the reading error in the fire emissions (see section 2.1.1). The generally only
3 moderate correlation coefficient is related to mismatches in the strong short-term variability
4 seen in both the model and the measurements.

5 The time series plots for stations in Europe, Asia and Canada in Fig. 9 demonstrate that the
6 annual CO cycle could to a large degree be reproduced correctly by the model with maximum
7 values occurring during the winter period and minimum values appearing during the summer
8 season. However, the model shows a negative offset during the winter period. Seasonal air
9 mass transport patterns that lead to regular annual re-occurring CO variations could be
10 reproduced for GAW stations in East Asia: The time series plots for Yonagunijima- YON and
11 Minamitorishima- MNM station, Japan (Fig. 9) show that the drop of CO, associated with the
12 air mass change from continental to cleaner marine air masses after the onset of the monsoon
13 season during the early summer months, is captured by the MACC_osuite. Deterioration in all
14 scores is visible during December 2010 in the time series plots of several stations (e.g.
15 Jungfrauoch-JFJ, and Sonnblick-SBL, Fig. 9). This is likely a result of changes in the
16 processing of the L2 IASI data and a temporary blacklisting of IASI data (to avoid model
17 failure) in the assimilation.

18 The comparison with MOPITT satellite CO total columns between October 2009 and June
19 2012 (described in section 2.2.3) shows a good qualitative agreement of spatial patterns and
20 seasonality, see Table 6. The MNMBs for 8 regions are listed in Fig. 13 and range between
21 ~~-22%~~ and ~~14%~~. The seasonality of the satellite observations is captured well by the
22 MACC_osuite over Asia and Africa, with MNMBs between -6% and 9% (North Africa),
23 -12% and 8% (South Africa), -11% and 12% (East Asia), and -3% and 14% (South Asia). The
24 largest negative MNMBs appear during the winter periods, especially from December 2010 to
25 May 2011 and from September 2011 to April 2012, for Alaska and Siberia and for the US and
26 Europe (MNMBs up to -22%), which coincides with large differences between MOPITT and
27 IASI satellite data (see Fig. 14). On the global scale the average difference between the IASI
28 and MOPITT total columns is less than 10% (George et al., 2009), and there is a close
29 agreement of MOPITT and IASI for S. Asia and Africa (see Fig. 14). However, larger
30 differences between MOPITT and IASI data appear during the northern winter months over
31 Alaska, Siberia, Europe and the US, which result in lower CO concentrations in the model,
32 due to the assimilation of IASI CO data in the MACC_osuite. The differences between

Gelöscht: 14%

Gelöscht: -22%.

1 MOPITT and IASI data can be mainly explained by the use of different a priori assumptions
2 in the IASI and MOPITT retrieval algorithms (George et al., 2015). Indeed, the Fast Optimal
3 Retrievals on Layers for IASI (FORLI) software (IASI) is using a single a priori CO profile
4 (with an associated variance-covariance matrix) whereas the MOPITT retrieval algorithm is
5 using a variable a priori, depending on time and location. George et al., (2015) show that
6 differences above Europe and the US in January and December (for a 5 year study) decrease
7 by a factor of 2 when comparing IASI with a modified MOPITT product using the IASI
8 single a priori. Between January 2011 and October 2011 there has also been a reading error in
9 the fire emissions that contributes to larger MNMBs during this period (see section 2.1.1).

Gelöscht: submitted

Gelöscht: (submitted)

Gelöscht: Tropospheric

Gelöscht: Nitrogen

Gelöscht: Dioxide

10 3.3 Evaluation of tropospheric nitrogen dioxide

11 Figure 15 shows global maps of daily tropospheric NO₂ VCD averaged from September 2009
12 to March 2012. Overall, spatial distribution and magnitude of tropospheric NO₂ observed by
13 SCIAMACHY are well reproduced by the model. This indicates that emission patterns and
14 NO_x photochemistry are reasonably well represented by the model. However, the model
15 underestimates tropospheric NO₂ VCDs over industrial areas in Europe, East China, Russia,
16 and South East Africa compared to satellite data. This could imply that anthropogenic
17 emissions from RETRO-REAS are too low in these regions, or that the lifetime in the model
18 is too short. The model simulates larger NO₂ VCD maxima over Central Africa, which mainly
19 originate from wild fires. It remains unclear if GFEDv2/GFAS fire emissions are too high
20 here or if NO₂ fire plumes closer to the ground cannot be seen by the satellites due to light
21 scattering by biomass burning aerosols (Leitao et al., 2010). In the northern hemisphere,
22 background values of NO₂ VCD over the ocean are lower in the simulations than in the
23 satellite data. The same is true for the South Atlantic Ocean to the west of Africa (see Fig.15).
24 This might suggest a model underestimation of NO₂ export from continental sources or too
25 rapid conversion of NO₂ into its reservoirs. However, as the NO₂ columns over the oceans are
26 close to the uncertainties in the satellite data, care needs to be taken when interpreting these
27 differences.

Gelöscht: underestimated

28 Time series of daily tropospheric NO₂ VCD averaged over different regions and
29 corresponding monthly means are presented in Figs. 16 and 17, respectively. Time series of
30 the MNMB and RMSE are shown in Figs. 18 and 19, respectively. Table 7 summarizes the
31 statistical values derived over the whole time period. High anthropogenic emissions occur
32 over the United States, Europe, South Asia and East Asia compared to other regions on the

1 globe (e.g., Richter et al., 2005). In principle, the MACC_osuite catches the pattern of
2 satellite NO₂ VCD over these regions. However, the model tends to underestimate NO₂ VCDs
3 throughout the whole time period investigated here. The negative bias is most pronounced
4 over East Asia with a modelled mean NO₂ VCD for September 2009 to December 2012 of
5 about 3.8×10^{15} molec cm⁻² lower than that derived from satellite measurements (see Table
6 7).

7 Considering monthly values, the MACC_osuite strongly underestimates magnitude and
8 seasonal variation of satellite NO₂ VCD over East Asia (MNMBs between about -40 % and
9 -110 % and RMSE between 1×10^{15} molec cm⁻² and 14×10^{15} molec cm⁻² throughout the
10 whole time period). A change in the modelled NO₂ values is apparent in July 2012 when the
11 emission inventories changed and the agreement with the satellite data improved for South
12 and East Asia but deteriorated for the US and Europe. This results in a drop of MNMBs (Fig.
13 18) for Europe and the US with values approaching around -70% by the end of 2012.
14 Nevertheless, correlations between daily satellite and model data derived for the whole time
15 period (see Table 7) are high for East Asia (0.8), South Asia (0.8), Europe (0.8), and lower,
16 but still rather high, for the US (0.6).

17 The North African and South African regions are strongly affected by biomass burning
18 (Schreier et al., 2013). Magnitude and seasonality of daily and monthly tropospheric NO₂
19 VCDs (Figs. 16 and 17, respectively) are rather well represented by the model, apart from
20 January 2011 to October 2011, due to difficulties in reading fire emissions for this time period
21 (see section 2.1.1). The latter results in large absolute values of the MNMB (Fig. 18) and
22 large RMSEs (Fig. 19) between January 2011 and October 2011 compared to the rest of the
23 time period. As for other regions investigated in this section, mean values of simulated daily
24 tropospheric NO₂ VCDs over North Africa and South Africa between September 2009 and
25 December 2012 tend to be lower than the corresponding satellite mean values (see Table 7).
26 The correlation between daily model and satellite data over the whole time period is about 0.6
27 for South Africa and 0.5 for North Africa. It should be investigated in future studies, if this
28 difference in model performance for the African regions is due to meteorology, chemistry or
29 emissions.

30 The evaluation of modelled NO₂ with GAW surface data for 6 European stations accordingly
31 shows that NO₂ is generally underestimated at the surface. MNMBs are typically in the range
32 of -26% and -45%. larger MNMBs appear only for two stations in complex mountainous

Formatiert: Tiefgestellt

Formatiert: Tiefgestellt

1 terrain (Rigi-RIG 68% and Sonnblick-SBL -160%). RMSEs are between 0.3 and 9 ppb,
2 correlation coefficients between 0.1 and 0.6 for the period between 9/2009 and 12/ 2012, see
3 Table 8. The annual cycle of NO₂ with maximum concentrations during the winter period is in
4 principle captured by the model, shown in the time series plots in Fig. 20. As is observed for
5 the satellite VCDs, NO₂ surface concentrations decrease in the model with the introduction of
6 the updated model version and emission inventories. For stations located in complex terrain
7 (e.g. Rigi, Fig. 20), results improve after the model update, likely also due to the higher model
8 resolution. Monthly values of MNMB, R and correlation coefficient are shown in Figs. 21 to
9 23.

Formatiert: Tiefgestellt

Formatiert: Tiefgestellt

11 4 Discussion

12 The validation of global O₃ mixing ratios with GAW observations at the surface levels
13 showed that the MACC_osuite could generally reproduce the observed annual cycle of ozone
14 mixing ratios. Model evaluation with surface data shows global average monthly MNMBs
15 between -30% and 30% (GAW) and for Europe between -50% and 60% (EMEP). For stations
16 located in the northern mid-latitudes, the evaluation reveals a seasonally dependent bias, with
17 an underestimation of the observed O₃ mixing ratios by the MACC osuite during the winter
18 season and an overestimation during the summer months. The validation of day-time versus
19 night-time concentrations for Northern and Central Europe shows larger negative MNMBs in
20 the winter months during night time than day time (Fig. 8), so that the negative bias in winter
21 could be attributed to the simulation of vertical mixing at night, also described by Ordoñez
22 (2010) and Schaap (2008), which remains a challenge in the model. The systematic
23 underestimation of O₃ mixing ratios throughout the year for high latitude northern regions and
24 Antarctica has its origin in an overestimation of the O₃ dry deposition velocities over ice.
25 With the implementation of the new model cycle and the updated MOZART model version,
26 which includes updated velocity fields for the dry deposition of O₃, as described in Stein et al.
27 (2013), the negative offset in the MACC_osuite model has been remedied for high latitude
28 regions from July 2012 onwards (see the time series plots for the South Pole station- SPO and
29 Neumayer- NEU in Fig. 3). The overestimation of O₃ mixing ratios during the summer
30 months is a well-known issue and has been described by various model validation studies
31 (e.g., Brunner et al., 2003, Schaap et al., 2008, Ordoñez et al., 2010, Val Martin et al., 2014).
32 Inadequate ozone precursor concentrations and aerosol induced radiative effects (photolysis)

Gelöscht: validation

Gelöscht: The bias between measured O₃ surface mixing ratios and the MACC_osuite

Gelöscht: is seasonally dependent

Gelöscht: northern

Gelöscht: ¶

Gelöscht: for

Gelöscht: northern hemisphere

1 have been frequently identified as being the main factors. The time series plots in Fig. 3,
2 however, demonstrate that the minimum concentrations in particular are not captured by the
3 model during summer. Possible explanations include a general underestimation of NO
4 titration which especially applies to stations with urban surroundings and strong sub-grid
5 scale emissions (e.g. Tsukuba-TSU Fig. 3), including difficulties by the global model to
6 resolve NO titration in urban plumes. It also seems likely that dry deposition at wet surfaces
7 in combination with the large surface sink gradient due to nocturnal stability cannot be
8 resolved with the model's vertical resolution. In regions such as Central and Southern Europe
9 (Fig. 8) where day time biases exceed night time biases, the overestimation of O₃ might be
10 related to an underestimation of day-time dry deposition velocities: Val Martin et al., (2014)
11 describe a reduction of the summertime O₃ model bias for surface ozone after the
12 implementation of adjustments in stomatal resistances in the MOZART model's dry
13 deposition parameterization.

14 The MACC_osuite model realistically reproduces CO total columns over most of the
15 evaluated regions with monthly MNMBs falling between 10% and -20% (Table 6). There is
16 | close agreement of modelled CO total columns and satellite observations for Africa and South
17 | Asia throughout the evaluation period. However, there is a negative offset compared to the
18 | observational CO data over Europe and North America. The largest deviations occur during
19 | the winter season when the observed CO concentrations are highest. The evaluation with
20 | GAW surface CO data accordingly shows a wintertime negative bias of up to -35% at the
21 | surface for stations in Europe and the US. A general underestimation of CO from global
22 | models in the northern hemisphere has been described by various authors (e.g., Shindell et al.,
23 | 2006, Naik et al., 2013). According to Stein et al. (2014) this underestimation likely results
24 | from a combination of errors in the dry deposition parameterization and certain limitations in
25 | the current emission inventories. The latter include too low anthropogenic CO emissions from
26 | traffic or other combustion processes and missing anthropogenic VOC emissions in the
27 | inventories together with an insufficiently established seasonality in the emissions. An
28 | additional reason for the apparent underestimation of emissions in MACCCity may be an
29 | exaggerated downward trend in the RCP8.5 (Representative Concentration Pathways)
30 | scenario in North America and Europe between 2000 and 2010, as this scenario was used to
31 | extrapolate the MACCCity emissions from their bench mark year, i.e. 2000. For CO,
32 | uncertainties in the evaluation also include the retrieved amount of CO total columns between
33 | IASI and MOPITT. These vary with region, with IASI showing lower CO concentrations in

Gelöscht: a

Gelöscht: at a

1 several regions (Alaska, Siberia, Europe and the US) during the northern winter months,
2 which possibly contribute to the deviations observed between the modelled data and MOPITT
3 satellite data, as only IASI data has been assimilated in the model. The differences can
4 primarily be explained by the use of different a priori assumptions in the IASI and MOPITT
5 retrieval algorithms (George et al., 2015). On a global scale however, the average difference
6 between the IASI and MOPITT total columns is less than 10% (George et al., 2009). From
7 July 2012 onwards, MOPITT CO total columns are also assimilated in the MACC_osuite.
8 Modelled NO₂ tropospheric columns agree well with satellite observations over the United
9 States, South Asia and North Africa. However, there is also a negative offset for NO₂ over
10 East Asia and Europe. For the latter, these findings are supported by the evaluation with
11 GAW surface data. Again, the largest deviations are occurring during the winter season. The
12 quality of the emission inventory is even more crucial for short lived reactive species such as
13 NO₂, where model results depend to a large extent on emission inventories incorporated in the
14 simulations. This is highlighted by the deterioration of agreement between model results and
15 satellite data for the US in July 2012 when anthropogenic emissions were changed from
16 RETRO-REAS to MACCcity. This change led to an increasing negative bias in NO₂ over
17 Europe and North America and to an improvement for South and East Asia (see Fig. 18). A
18 deterioration in MNMBs associated with the fire emissions is visible between January 2011
19 and October 2011 over regions with heavy fire activity (Africa and East Asia), and goes back
20 to a temporary error in the model regarding the reading of fire emissions (see Figs. 17 and
21 18). Particular challenges for an operational forecast system are regions with rapid changes in
22 emissions such as China, where inventories need to be extrapolated to obtain reasonable
23 trends. A large underestimation of NO₂ in China especially in winter has been reported for
24 other CTMs in previous publications (He et al., 2007, Itahashi et al., 2014). The latter has
25 been linked to an underestimation of NO_x and VOC emissions, unresolved seasonality in the
26 emissions and expected non-linearity of NO_x chemistry. The change in validation data sets
27 from SCIAMACHY to GOME-2 has shown to have negligible impact on the validation
28 results and conclusions.

Gelöscht: submitted

Gelöscht: ¶

Gelöscht: total

Gelöscht:

Gelöscht: and East Asia.

29

30 5 Conclusion

31 The MACC_osuite is the global near-real-time MACC model analysis run for aerosol and
32 reactive gases. The model has been evaluated with surface observations and satellite data

1 concerning its ability to simulate reactive gases in the troposphere. Results showed that the
2 model proved capable of a realistic reproduction of the observed annual cycle for CO, NO₂
3 and O₃ mixing ratios at the surface, however, with seasonally dependent biases. For ozone,
4 these seasonal biases likely result from difficulties in the simulation of vertical mixing at
5 night and deficiencies in the model's dry deposition parameterization. For CO, a negative
6 offset in the model during the winter season is attributed to limitations in the emission
7 inventories together with an insufficiently established seasonality in the emissions.

Formatiert: Tiefgestellt

8 NO₂ total columns derived from satellite sensors and surface NO₂ observed by European
9 GAW stations could be reproduced reasonably well over most of the evaluated regions, but
10 showed a negative offset compared to the observational data, especially over Europe and East
11 Asia (NO₂). It has become clear, that the emission inventories play a crucial role for the
12 quality of model results and remain a challenge for near-real-time modeling, especially over
13 regions with rapid changes in emissions. Inconsistencies in the assimilated satellite data and
14 fire emissions showed only a temporary impact on the quality of model results. The
15 implementation of a model update improved the results especially in the high latitudes
16 (surface ozone) and over South and East Asia (NO₂).

Gelöscht: CO and

Formatiert: Tiefgestellt

Gelöscht:

Gelöscht: and North America
(CO) and over Europe

Gelöscht: that

Gelöscht:

17 The MACC NRT forecast system is constantly evolving. A promising step in model
18 development is the on-line integration of modules for atmospheric chemistry in the IFS,
19 currently being tested for implementation in the MACC_osuite. In contrast to the coupled
20 model configuration as used in this paper, the on-line integration in the Composition IFS (C-
21 IFS) provides major advantages; apart from an enhanced computational efficiency, C-IFS
22 promises an optimization of the implementation of feedback processes between gas-
23 phase/aerosol chemical processes and atmospheric composition and meteorology, which is
24 expected to improve the modeling results for reactive gases. Additionally, C-IFS will be
25 available in combination with different CTMs, (MOZART and TM5), which will help to
26 explain whether deviations between model and observations go back to deficiencies in the
27 chemistry scheme of a model.

Formatiert: Tiefgestellt

Gelöscht: ¶

28 Acknowledgements

29 This work has been carried out in the framework of the MACC projects, funded under the EU
30 Seventh Research Framework Programme for research and technological development. The
31 authors thank the MACC validation and reactive gas subproject teams for the fruitful
32 discussions. Model simulations were carried out using the ECMWF supercomputer. We wish

1 to acknowledge the provision of GAW hourly station data from the World Data Centre of
2 Greenhouse Gases (WDCGG) and hourly EMEP station data from the NILU database.
3 Specifically, we like to thank: the CSIRO Oceans and Atmosphere Flagship for making the
4 data freely available and the Australian Bureau of Meteorology for continued operation and
5 support of the Cape Grim station. We also like to thank Izaña Atmospheric Research Center
6 (AEMET) for providing CO and O₃ data. Special thanks to the providers of NRT data to the
7 MACC project, namely: Institute of Atmospheric Sciences and Climate (ISAC) of the Italian
8 National Research Council (CNR), South African Weather Service, The University of York
9 and National Centre for Atmospheric Science (NCAS (AMF)) (UK), and the Instituto
10 Nacional de Meteorologia e Geofisica (INMG) (Cape Verde), National Air Pollution
11 Monitoring Network (NABEL) (Federal Office for the Environment FOEN and Swiss Federal
12 Laboratories for Materials Testing and Research EMPA), Japan Meteorological Agency
13 (JMA), Alfred Wegener Institute, Umweltbundesamt (Austria), National Meteorological
14 Service (Argentina), Umweltbundesamt (UBA, Germany). We thank the National Center for
15 Atmospheric Research (NCAR) MOPITT science team and the NASA Langley Research
16 Center, Atmospheric Science Data Center (ASDC), for producing and archiving the MOPITT
17 CO product. IASI has been developed and built under the responsibility of the Centre
18 National D'Etudes Spatiales (CNES, France). We are grateful to Juliette Hadji-Lazaro and the
19 UBL/ LATMOS IASI team for establishing the IASI-MACC near real time processing chain.
20 We wish to acknowledge that SCIAMACHY lv1 (level 1) radiances were provided to the
21 Institute of Environmental Physics, University of Bremen by ESA through DLR/DFD.

22 **References**

- 23 Aas, W., Hjellbrekke, A.-G., Schaug, J.: Data quality 1998, quality assurance and field
24 comparisons. Kjeller, Norwegian Institute for Air Research (EMEP/CCC-Report 6/2000),
25 2000.
- 26 Ashmore, M. R.: Assessing the future global impacts of ozone on vegetation. *Plant Cell*
27 *Environ.* 28, 949–964, 2005.
- 28 Ballabrera-Poy, J., Kalnay, E. and Yang, S.: Data assimilation in a system with two
29 scales—combining two initialization techniques. *Tellus* (2009), 61A, 539–549,
30 doi:10.1111/j.1600-0870.2009.00400.x, 2009.
- 31 Bell M.L., R.D. Peng and F. Dominici: The exposure–response curve for O₃ and risk of
32 mortality and the adequacy of current O₃ regulations. *Environmental Health Perspectives*,

1 114 (4), 2006.

2 Benedetti, A., Morcrette, J.-J., Boucher, O., Dethof, A., Engelen, R. J., Fisher, M., Flentje, H.,
3 Huneus, N., Jones, L., Kaiser, J. W., Kinne, S., Mangold, A., Razinger, M., Simmons, A. J.,
4 Suttie, M., and the GEMS-AER team: Aerosol analysis and forecast in the European Centre
5 for Medium-Range Weather Forecasts Integrated Forecast System: Data Assimilation. *J.*
6 *Geophys. Res.*, D13205, 114, doi:10.1029/2008JD011115, 2008.

7 Benedetti, A., Kaiser, J. W., and Morcrette J.-J.: [Global Climate] Aerosols [in "State of the
8 Climate in 2010"]. *B. Am.Meterol. Sci.*, 92(6):S65–S67, 2011.

9 Boersma, K.F., Eskes, H.J., Brinksma, E.J.: Error analysis for tropospheric NO₂ retrieval
10 from space. *J. Geophys. Res.*, 109, D4, doi:10.1029/2003JD003962, 2004.

11 Bovensmann, H., J. P. Burrows, M. Buchwitz, J. Frerick, S. Noël, V. V. Rozanov, K. V.
12 Chance, A. P. H. Goede: *SCIAMACHY: Mission Objectives and Measurement Modes*. *J.*
13 *Atmos. Sci.*, 56, 127–150, 1999.

14 Brunner, D., Staehelin, J., Rogers, H. L., Köhler, M. O., Pyle, J. A., Hauglustaine, D.,
15 Jourdain, L., Berntsen T. K., Gauss, M., Isaksen, I. S. A., Meijer, E., van Velthoven, P.,
16 Pitari, G., Mancini, E., Grewe, V. and Sausen, R.: An evaluation of the performance of
17 chemistry transport models by comparison with research aircraft observations. Part 1:
18 Concepts and overall model performance. *Atmos. Chem. Phys.*, 3, 1609–1631,
19 doi:10.5194/acp-3-1609-2003, 2003.

20 Callies, J., Corpaccioli, E., Eisinger, M., Hahne, A., and Lefebvre, A.: GOME-2 Metop's
21 Second-Generation Sensor for Operational Ozone Monitoring, *ESA Bull.*, 102, 28–36, 2000.

22 Cammas, J.-P., A. Gilles, S. Chabrillat, F. Daerden, N. Elguindi, J. Flemming, H. Flentje, C.
23 Deshler, T., J.L. Mercer, H.G.J. Smit, R. Stubi, G. Levrat, B.J. Johnson, S.J. Oltmans, R.
24 Kivi, A.M. Thompson, J. Witte, J. Davies, F.J. Schmidlin, G. Brothers, T. Sasaki
25 Atmospheric comparison of electrochemical cell ozonesondes from different manufacturers,
26 and with different cathode solution strengths: The Balloon Experiment on Standards for
27 Ozonesondes. *J. Geophys. Res.*113, D04307, doi:10.1029/2007JD008975, 2008.

28 Cape, J.N.: Surface ozone concentrations and ecosystem health: Past trends and a guide to
29 future projections. *Science of the Total Environment* Vol. 400, 257-269.,
30 doi:10.1016/j.scitotenv.2008.06.025, 2008.

1 Clarisse, L., R'Honi, Y., Coheur, P.-F., Hurtmans, D., and Clerbaux, C.: Thermal infrared
2 nadir observations of 24 atmospheric gases, *Geophys. Res. Lett.*, 38, L10802,
3 doi:10.1029/2011GL047271, 2011.

4 Clerbaux, C., Boynard, A., Clarisse, L., George, M., Hadji-Lazaro, J., Herbin, H., Hurtmans,
5 D., Pommier, M., Razavi, A., Turquety, S., Wespes, C., and Coheur, P.-F.: Monitoring of
6 atmospheric composition using the thermal infrared IASI/MetOp sounder, *Atmos. Chem.*
7 *Phys.*, 9, 6041–6054, doi:10.5194/acp-9-6041-2009, 2009.

8 Cooper, O. R., Parrish, D. D., Ziemke, J., Balashov, N. V., Cupeiro, M., Galbally, I. E., Gilge,
9 S., Horowitz, L., Jensen, N. R., Lamarque, J.-F., Naik, V., Oltmans, S. J., Schwab, J.,
10 Shindell, D. T., Thompson, A. M., Thouret, V., Wang, Y., Zbinden, R. M.: Global
11 distribution and trends of tropospheric ozone: an observation-based review, *Elem. Sci. Anth.*,
12 2,10 000029, doi:10.12952/journal.elementa.000029, 2014.

13 Cuevas, E., Camino, C., Benedetti, A., Basart, S., Terradellas, E., Baldasano, J.M., Morcrette,
14 J.-J., Marticorena, B., Goloub, P., Mortier, A., Berjón, A., Hernández, Y., Gil-Ojeda, M.,
15 Schulz, M.: The MACC-II 2007-2008 Reanalysis: Atmospheric Dust Evaluation and
16 Characterization over Northern Africa and Middle East, *Atmos. Chem. Phys.* 15, 3991–4024,
17 doi:10.5194/acp-15-3991-2015, 2015.

18 Deeter, M. N., Emmons, L. K., Edwards, D. P., Gille, J. C., and Drummond, J. R.: Vertical
19 resolution and information content of CO profiles retrieved by MOPITT, *Geophys. Res. Lett.*,
20 31, L15112, doi:10.1029/2004GL020235, 2004.

21 Deeter, M. N., et al.: The MOPITT version 4 CO product: Algorithm enhancements,
22 validation, and long-term stability, *J. Geophys. Res.*, 115, D07306,
23 doi:10.1029/2009JD013005, 2010.

24 Deeter, M. N., H. M. Worden, D. P. Edwards, J. C. Gille, D. Mao, and J. R. Drummond:
25 MOPITT multispectral CO retrievals: Origins and effects of geophysical radiance errors, *J.*
26 *Geophys. Res.*, 116, doi:10.1029/2011JD015703, 2011.

27 Deeter, M. N., Worden, H. M., Edwards, D. P., Gille, J. C., Andrews, A. E.: evaluation of
28 MOPITT retrievals of lower-tropospheric carbon monoxide over the United States, *J.*
29 *Geophys. Res.*, 117, D13306, doi:10.1029/2012JD017553, 2012.

30 Deeter, M. N., Martínez-Alonso, S., Edwards, D. P., Emmons, L. K., Gille, J. C., Worden, H.
31 M., Pittman, J. V., Daube, B. C., Wofsy, S. C.: Validation of MOPITT Version 5 thermal-

1 infrared, near-infrared, and multispectral carbon monoxide profile retrievals for 2000–2011, J.
 2 Geophys. Res. Atmos., 118, 6710–6725, doi:10.1002/jgrd.50272, 2013.

3 De Wachter, E., Barret, B., Le Flochmoën, E., Pavelin, E., Matricardi, M., Clerbaux, C.,
 4 Hadji-Lazaro, J., George, M., Hurtmans, D., Coheur, P.-F., Nedelec, P., and Cammas, J. P.:
 5 Retrieval of MetOp-A/IASI CO profiles and validation with MOZAIC data, Atmos. Meas.
 6 Tech., 5, 2843-2857, doi:10.5194/amt-5-2843-2012, 2012.

7 Drummond, J. R. and Mand, G. S.: The Measurements of Pollution in the Troposphere
 8 (MOPITT) Instrument: Overall Performance and Calibration Requirements. J. Atmos.
 9 Oceanic Technol., 13, 314–320, 1996.

10 Elguindi, N., Clark, H., Ordóñez, C., Thouret, V., Flemming, J., Stein, O., Huijnen, V.,
 11 Moinat, P., Inness, A., Peuch, V.-H., Stohl, A., Turquety, S., Athier, G., Cammas, J.-P., and
 12 Schultz, M.: Current status of the ability of the GEMS/MACC models to reproduce the
 13 tropospheric CO vertical distribution as measured by MOZAIC, Geosci. Model Dev., 3, 501-
 14 518, doi:10.5194/gmd-3-501-2010, 2010.

15 Emmons, L. K., Edwards, D. P., Deeter, M. N., Gille, J. C., Campos, T., Nédélec, P.,
 16 Novelli, P. and G. Sachse: Measurements of Pollution In The Troposphere (MOPITT)
 17 validation through 2006, Atmos. Chem. Phys., 9(5), 1795–1803, doi:10.5194/acp-9-1795-
 18 2009, 2009.

19 Engelen R. J., Serrar, S., Chevallier, F.: Four-dimensional data assimilation of atmospheric
 20 CO₂ using AIRS observations, J. Geophys. Res., 114, D03303, doi:10.1029/2008JD010739,
 21 2009.

22 [Eskes, H., Huijnen, V., Arola, A., Benedictow, A., Blechschmidt, A.-M., Botek, E., Boucher,](#)
 23 [O., Bouarar, I., Chabrillat, S., Cuevas, E., Engelen, R., Flentje, H., Gaudel, A., Griesfeller, J.,](#)
 24 [Jones, L., Kapsomenakis, J., Katragkou, E., Kinne, S., Langerock, B., Razinger, M., Richter,](#)
 25 [A., Schultz, M., Schulz, M., Sudarchikova, N., Thouret, V., Vrekoussis, M., Wagner, A., and](#)
 26 [Zerefos, C.: Validation of reactive gases and aerosols in the MACC global analysis and](#)
 27 [forecast system. Geosci. Model Dev. Discuss., 8, 1117-1169, doi:10.5194/gmdd-8-1117-](#)
 28 [2015, 2015.](#)

29 Flemming, J., and Inness, A., Volcanic sulfur dioxide plume forecasts based on UV satellite
 30 retrievals for the 2011 Grímsvötn and the 2010 Eyjafjallajökull eruption, Journal of
 31 Geophysical Research: Atmospheres 118, 10172-10189, doi:10.1002/jgrd.50753, 2013.

Formatiert: Schriftart: 12 pt,
 Schriftartfarbe: Schwarz,
 Englisch (USA)

Formatiert: Schriftart: 12 pt,
 Schriftartfarbe: Schwarz,
 Englisch (USA)

Formatiert: Zeilenabstand: 1,5
 Zeilen

Formatiert: Schriftart: 12 pt,
 Schriftartfarbe: Schwarz,
 Englisch (USA)

Formatiert: Schriftart: 12 pt,
 Schriftartfarbe: Schwarz,
 Englisch (USA)

Formatiert: Schriftart: 12 pt,
 Schriftartfarbe: Schwarz,
 Englisch (USA)

Formatiert: Schriftart: 12 pt,
 Schriftartfarbe: Schwarz,
 Englisch (USA)

Formatiert: Englisch (USA)

1 Flemming, J., Inness, A., Flentje, H., Huijnen, V., Moinat, P., Schultz, M.G., Stein, O.:
2 Coupling global chemistry transport models to ECMWF's integrated forecast system, *Geosci.*
3 *Model Dev.*, 2, 253-265, doi:10.5194/gmd-2-253-2009, 2009.

4 Forster, P., V. Ramaswamy, P. Artaxo, T. Berntsen, R. Betts, D.W. Fahey, J. Haywood, J.
5 Lean, D.C. Lowe, G. Myhre, J. Nganga, R. Prinn, G. Raga, M. Schulz and R. Van Dorland:
6 Changes in Atmospheric Constituents and in Radiative Forcing. In: *Climate Change 2007:*
7 *The Physical Science Basis. Contribution of Working Group I to the Fourth Assessment*
8 *Report of the Intergovernmental Panel on Climate Change* [S. Solomon, D. Qin, M. Manning,
9 Z. Chen, M. Marquis, K.B. Averyt, M. Tignor and H.L. Miller (eds.)]. USA, 2007.

10 George, M., Clerbaux, C., Hurtmans, D., Turquety, S., Coheur, P.-F., Pommier, M., Hadji-
11 Lazaro, J., Edwards, D. P., Worden, H., Luo, M., Rinsland, C., and McMillan, W.: Carbon
12 monoxide distributions from the IASI/METOP mission: evaluation with other space-borne
13 remote sensors, *Atmos. Chem. Phys.*, 9, 8317–8330, doi:10.5194/acp-9-8317-2009, 2009.

14 George, M., Clerbaux, C., Bouarar, I., Coheur, P.-F., Deeter, M. N., Edwards, D. P., Francis,
15 G., Gille, C., Hadji-Lazaro, J., Hurtmans, D., Inness, A., Mao, D., Worden H. M.: An
16 examination of the long-term CO records from MOPITT and IASI and comparison of
17 retrieval methodology, [Atmos. Meas. Tech.](https://doi.org/10.5194/amt-8-4313-2015), 8, 4313-4328, doi:10.5194/amt-8-4313-2015,
18 [2015](https://doi.org/10.5194/amt-8-4313-2015).

19 Gomez-Pelaez, A. J., Ramos, R., Gomez-Trueba, V., Novelli, P. C., and Campo-Hernandez,
20 R.: A statistical approach to quantify uncertainty in carbon monoxide measurements at the
21 Izaña global GAW station: 2008–2011, *Atmos. Meas. Tech.*, 6, 787-799, doi:10.5194/amt-6-
22 787-2013, 2013.

23 Granier, C., Huijnen, V., Inness, A., Jones, L., Katragkou E., Khokhar, F., Kins, L., Law, K.,
24 Lefever, K., Leitao, J., Melas, D., Moinat, P., Ordonez, C., Peuch, V.-H., Reich, G., Schultz,
25 M., Stein, O., Thouret, V., Werner, T., Zerefos, C., GEMS GRG Comprehensive Validation
26 Report. Available as project report at <http://gems.ecmwf.int> (last access: February 2015),
27 2009.

28 Granier, C., Bessagnet, B., Bond, T., D'Angiola, A., van der Gon, H. D., Frost, G. J., Heil, A.,
29 Kaiser, J. W., Kinne, S., Klimont, Z., Kloster, S., Lamarque, J.-F., Liousse, C., Masui, T.,
30 Meleux, F., Mieville, A., Ohara, T., Raut, J. C., Riahi, K., Schultz, M. G., Smith, S. J.,
31 Thompson, A., van Aardenne, J., van der Werf, G. R., and van Vuuren, D. P.: Evolution of
32 anthropogenic and biomass burning emissions of air pollutants at global and regional scales

Gelöscht: Atmos. Meas. Tech.
Discuss., submitted, 2015.¶

1 during the 1980–2010 period, *Climatic Change*, 109, 163–190, doi:10.1007/s10584-011-
2 0154-1, 2011.

3 Griffin, R.J., Chen, J., Carmody, K. and Vutukuru, S.: Contribution of gas phase oxidation of
4 volatile organic compounds to atmospheric carbon monoxide levels in two areas of the united
5 States. *J. Geophys. Res.*, 11, D10S17, doi:10.1029/2006JD007602, 2007.

6 Guenther, A., Karl, T., Harley, P., Wiedinmyer, C., Palmer, P.I., and Geron, C.: Estimates of
7 global terrestrial isoprene emissions using MEGAN (Model of Emissions of Gases and
8 Aerosols from Nature), *Atmos. Chem. Phys.*, 6, 3181-3210, doi:10.5194/acp-6-3181-2006,
9 2006.

10 He, Y, Uno, I, Wang, Z., Ohara, T., Sugimoto, N., Shimizu, A., Richter, A., Burrows, J. P.:
11 Variations of the increasing trend of tropospheric NO₂ over central east China during the past
12 decade, *Atmospheric Environment*, 41, 4865–4876, 2007.

13 Hilboll, A., Richter, A., and Burrows, J.P.: Long-term changes of tropospheric NO₂ over
14 megacities derived from multiple satellite instruments, *Atmos. Chem. Phys.*, 13, 4145-4169,
15 doi:10.5194/acp-13-4145-2013, 2013a.

16 Hilboll, A., Richter, A., Rozanov, A., Hodnebrog, Ø., Heckel, A., Solberg, S., Stordal, F.,
17 and Burrows, J.P.: Improvements to the retrieval of tropospheric NO₂ from Satellite –
18 stratospheric correction using SCIAMACHY limb/nadir matching and comparison to Oslo
19 CTM2 simulations. *Atmos. Meas. Tech.*, 6, 565–584. doi:10.5194/amt-6-565-2013, 2013,
20 2013b.

21 Hollingsworth, A., Engelen, R.J., Benedetti, A., Dethof, A., Flemming, J., Kaiser, J.W.,
22 Simmons, A.J.: Toward a monitoring and forecasting system for atmospheric composition:
23 The GEMS project, *B.Am. Meteor. Soc.*, 89, 1147–1164, doi:[10.1175/2008BAMS2355.1](https://doi.org/10.1175/2008BAMS2355.1),
24 2008.

25 Hudman, R.C., Murray, L.T., Jacob, D.J., Millet, D.B., Turquety, S., Wu, S., Blake, D.R.,
26 Goldstein, A.H., Holloway, J., Sachse, G.W.: Biogenic versus anthropogenic sources of CO
27 over the United States. *Geophys. Res. Lett.*, 35, L04801, doi:10.1175/2007GL032393, 2008.

28 Huijnen, V., Williams, J., vanWeele, M., van Noije, T., Krol, M., Dentener, F., Segers, A.,
29 Houweling, S., Peters, W., de Laat, J., Boersma, F., Bergamaschi, P., van Velthoven, P., Le
30 Sager, P., Eskes, H., Alkemade, F., Scheele, R., Nédélec, P., and Pätz, H.-W.: The global

1 chemistry transport model TM5: description and evaluation of the tropospheric chemistry
2 version 3.0, *Geosci. Model Dev.*, 3, 445–473, doi:10.5194/gmd-3-445-2010, 2010.

3 Huijnen, V., Flemming, J., Kaiser, J. W., Inness, A., Leitao, J., Heil, A., Eskes, H. J., Schultz,
4 M. G., Benedetti, A., Dufour, G., and Eremenko, M., Hindcast experiments of tropospheric
5 composition during the summer 2010 fires over Western Russia, *Atmos. Chem. Phys.* 12,
6 4341-4364, doi:10.5194/acp-12-4341-2012, 2012.

7 Hurtmans, D., Coheur, P.-F., Wespes, C., Clarisse, L., Scharf, O., Clerbaux, C., Hadji-Lazaro,
8 J., George, M., and Turquety, S.: FORLI radiative transfer and retrieval code for IASI. *J*
9 *Quant Spectrosc Radiat Transfer*, 113, 1391–1408, doi:10.1016/j.jqsrt.2012.02.036, 2012.

10 Inness, A., Flemming, J., Suttie, M. and Jones, L.: GEMS data assimilation system for
11 chemically reactive gases. ECMWF RD Tech Memo 587. Available from
12 <http://www.ecmwf.int>. (last access: February 2015), 2009.

13 Inness, A., F. Baier, F., 2, Benedetti, A., Bouarar, I., Chabrillat, S., Clark, H., Clerbaux, C.,
14 Coheur, P., Engelen, R. J., Errera, Q., Flemming, J., George, M., Granier, C., Hadji-Lazaro,
15 J., Huijnen, V., Hurtmans, D., Jones, L., Kaiser, J. W., Kapsomenakis, J., Lefever, K., Leitão
16 J., Razinger, M., Richter, A., Schultz, M. G., Simmons, A. J., Suttie, M., Stein O., Thépaut J.-
17 N., Thouret, V., Vrekoussis, M., Zerefos, C., al.: The MACC reanalysis: an 8 yr data set of
18 atmospheric composition, *Atmos. Chem. Phys.* 13, 4073–4109, doi:10.5194/acp-13-4073-
19 2013, 2013.

20 Inness, A., Blechschmidt, A.-M., Bouara, I., Chabrillat, S., Crepulja, M., Engelen, R. J.,
21 Eskes, H., Flemming, J., Gaudel, A., Hendrick, F., Huijnen, V., Jones, L., Kapsomenakis, J.,
22 Katragkou, E., Keppens, A., Langerock, B., de Mazière, M., Melas, D., M. Parrington, V.H.
23 Peuch, M. Razinger, A. Richter, M.G. Schultz, M. Suttie, V. Thouret, Vrekoussis, M.,
24 Wagner, A., and Zerefos C.: Data assimilation of satellite retrieved ozone, carbon monoxide
25 and nitrogen dioxide with ECMWF's Composition-IFS. *Atmos. Chem. Phys.*, 15, 1–29,
26 2015. doi:10.5194/acp-15-1-2015.

27 Itahashi, S., Uno, I., Irie, H., Kurokawa, J.-I., and Ohara, T.: Regional modeling of tropospheric
28 NO₂ vertical column density over East Asia during the period 2000–2010: comparison with
29 multisatellite observations, *Atmos. Chem. Phys.*, 14, 3623-3635, doi:10.5194/acp-14-3623-
30 2014, 2014.

Formatiert: Tiefgestellt

1 Kaiser, J. W., Heil, A., Andreae, M. O., Benedetti, A., Chubarova, N., Jones, L., Morcrette,
2 J.-J., Razinger, M., Schultz, M. G., Suttie, M., and van der Werf, G. R.: Biomass burning
3 emissions estimated with a global fire assimilation system based on observed fire radiative
4 power. *Biogeosciences*, 9, 527–554, doi:10.5194/bg-9-527-2012, 2012.

5 Kalnay, E., M. Kanamitsu, R. Kistler, W. Collins, D. Deaven, L. Gandin, M. Iredell, S. Saha,
6 G. White, J. Woollen, Y. Zhu, M. Chelliah, W. Ebisuzaki, W. Higgins, J. Janowiak, K. C.
7 Mo, C. Ropelewski, J. Wang, A. Leetmaa, R. Reynolds, R. Jenne, and D. Joseph: The
8 NCEP/NCAR 40-Year Reanalysis Project. *Bull. Amer. Meteor. Soc.*, 77, 437–471,
9 doi:[http://dx.doi.org/10.1175/1520-0477\(1996\)077<0437:TNYRP>2.0.CO;2](http://dx.doi.org/10.1175/1520-0477(1996)077<0437:TNYRP>2.0.CO;2), 1996.

10 Kalnay, E.: *Atmospheric Modeling, Data Assimilation and Predictability*. Cambridge
11 University Press, 2003.

12 Kampa, M. and Castanas, E.: Human health effects of air pollution. *Environmental*
13 *Pollution* Volume 151, Issue 2, 362–367, 2008.

14 Kerzenmacher, T., Dils, B., Kumps, N., Blumenstock, T., Clerbaux, C., Coheur, P.-F.,
15 Demoulin, P., García, O., George, M., Griffith, D. W. T., Hase, F., Hadji-Lazaro, J.,
16 Hurtmans, D., Jones, N., Mahieu, E., Notholt, J., Paton-Walsh, C., Raffalski, U., Ridder, T.,
17 Schneider, M., Servais, C., and De Mazière, M.: Validation of IASI FORLI carbon monoxide
18 retrievals using FTIR data from NDACC, *Atmos. Meas. Tech.*, 5, 2751–2761,
19 doi:10.5194/amt-5-2751-2012, 2012.

20 Kinnison, D. E., Brasseur, G. P., Walters, S., Gracia, R. R., Marsh, D. R., Sassi, F., Harvey,
21 V. L., Randall, C.E., Emmons, L., Lamarque, J. F., Hess, P., Orlando, J. J., Tie, X. X.,
22 Randel, W., Pan, L. L., Gettelman, A., Granier, C., Diehl, T., Niemeier, U. and Simmons, A.
23 J.: Sensitivity of chemical tracers to meteorological parameters in the MOZART-3 chemical
24 transport model. *J. Geophys. Res.*, 112, D20302, doi:10.1029/2006JD007879, 2007.

25 Lefever, K., van der A, R., Baier, F., Christophe, Y., Errera, Q., Eskes, H., Flemming, J.,
26 Inness, A., Jones, L., Lambert, J.-C., Langerock, B., Schultz, M. G., Stein, O., Wagner, A.,
27 and Chabrillat, S.: Copernicus atmospheric service for stratospheric ozone: validation and
28 intercomparison of four near real-time analyses, 2009–2012, *Atmos. Chem. Phys. Discuss.*,
29 14, 12461-12523, doi:10.5194/acpd-14-12461-2014, 2014.

1 Leitão, J., Richter, A., Vrekoussis, M., Kokhanovsky, A., Zhang, Q. J., Beekmann, M., and
2 Burrows, J. P.: On the improvement of NO₂ satellite retrievals – aerosol impact on the air mass
3 factors, *Atmos. Meas. Tech.*, 3, 475-493, doi:10.5194/amt-3-475-2010, 2010.

4 Leue, C., Wenig, M., Wagner, T., Platt, U. & Jähne, B. Quantitative analysis of NO_x
5 emissions from GOME satellite image sequences. *J. Geophys. Res.*, 106, 5493–5505, 2001.

6 Massart, S., Agusti-Panareda, A., Aben, I., Butz, A., Chevallier, F., Crevosier, C., Engelen,
7 R., Frankenberg, C., and Hasekamp, O.: Assimilation of atmospheric methane products into
8 the MACC-II system: from SCIAMACHY to TANSO and IASI. *Atmos. Chem. Phys.*, 14,
9 6139-6158, doi:10.5194/acp-14-6139-2014, 2014.

10 Mohnen, V.A., Goldstein, and Wang, W.-C.: Tropospheric Ozone and Climate Change, *Air &*
11 *Waste*, 43:10, 1332-1334, doi:10.1080/1073161X.1993.10467207, 1993.

12 Morcrette, J.-J., Boucher, O., Jones, L., Salmond, D., Bechthold, P., Beljaars, A., Benedetti,
13 A., Bonet, A., Kaiser, J.W., Razinger, M., Schulz, M., Serrar, S., Simmons, A.J., Sofiev, M.,
14 Suttie, M., Tompkins, A.M., Untch, A.: Aerosol analysis and forecast in the European Centre
15 for Medium- Range Weather Forecasts Integrated Forecast System: forward modeling, *J.*
16 *Geophys. Res.*, 114, D06206, doi:10.1029/2008JD011235, 2009.

17 Naik, V., Voulgarakis, A., Fiore, M., Horowitz, L.W., Lamarque, J.-F., Lin, M., Prather, M.
18 J., Young, P. J., Bergmann, D., Cameron-Smith, P. J., Cionni I., Collins W. J., Dalsøren, S.
19 B., Doherty, R., Eyring V., Faluvegi, G., Folberth, G. A., Josse, B., Lee, Y. H., MacKenzie, I.
20 A., Nagashima, T., van Noije, T. P. C., Plummer, D. A., Righi, M., Rumbold, S. T., Skeie, R.
21 D., Shindell, T., Stevenson, D. S., Strode, S., Sudo, K., Szopa, S., and Zeng, G. : Preindustrial
22 to present-day changes in tropospheric hydroxyl radical and methane lifetime from the
23 Atmospheric Chemistry and Climate Model Intercomparison Project (ACCMIP). *Atmos.*
24 *Chem. Phys.*, 13, 5277–5298, doi:10.5194/acp-13-5277-2013, 2013.

25 Novelli, P.C., Masarie, K.A. and Lang, P.M.: Distributions and recent changes of carbon
26 monoxide in the lower troposphere, *J. Geophys. Res.*, 103, 19015-19033,
27 doi:10.1029/98JD01366, 1998.

28 Ordoñez, C., Elguindi, N., Huijnen, V., Flemming, J., Inness, A., Flentje, H., Katragkou, E.,
29 Moinat, P., Peuch, V.-H., Segers, A., Thouret, V., Athier, G., van Weele, M., Zerefos, C.s.,
30 Cammas, J.-P., Schulz, M.G.: Global Model simulations of air pollution during the 2003
31 European heat wave. *Atmos. Chem. Phys.*, 10, 789-815, doi:10.5194/acp-10-789-2010, 2010.

- 1 Park, R.J., Pickering, K.E., Allen, D. J : Global simulation of tropospheric ozone using the
2 University of Maryland Chemical Transport Model (UMD-CTM): 1. model description and
3 evaluation. *J. Geophys. Res.*, 109, doi:101029/2003JD004266, 2004.
- 4 Penkett, S., Gilge, S., Plass-Duelmer, C. Galbally, I.: WMO/GAW Expert Workshop on
5 Global Long-term Measurements of Nitrogen Oxides and Recommendations for GAW
6 Nitrogen Oxides Network, WMO, Geneva, 2011.
- 7 Platt, U., and Stutz, J.: Differential Optical Absorption Spectroscopy. *Physics of Earth and*
8 *Space Environments*. Berlin: Springer, [http://www.springerlink.com/content/978-3-540-](http://www.springerlink.com/content/978-3-540-21193-8)
9 [21193-8](http://www.springerlink.com/content/978-3-540-21193-8) (last access: February. 2015), 2008.
- 10 Richter, A., and Burrows, J.P.: “Tropospheric NO₂ from GOME Measurements.” *Advances in*
11 *Space Research* 29, no. 1, 1673–1683. doi:10.1016/S0273-1177(02)00100-X, 2002.
- 12 Richter, A., Burrows, J. P., Nüß, H., Granier, C, Niemeier, U.: Increase in tropospheric
13 nitrogen dioxide over China observed from space, *Nature*, 437-132,doi:10.1038/nature04092,
14 2005.
- 15 Richter, A. Begoin, M., Hilboll, A., and Burrows, J. P.: An improved NO₂ retrieval for the
16 GOME-2 satellite instrument, *Atmos. Meas. Tech.*, 4, 1147-1159, doi:10.5194/amt-4-1147-
17 2011, 2011.
- 18 Rodgers, C. D.: *Inverse Methods for Atmospheric Sounding, Theory and Practice*, World
19 Scientific, Singapore, 2000.
- 20 Rozanov, A., Vladimir V., Rozanov, M., Buchwitz, A., Kokhanovsky, A. and Burrows, J.P.:
21 “SCIATRAN 2.0 - A New Radiative Transfer Model for Geophysical Applications in the
22 175-2400 Nm Spectral Region.” *Advances in Space Research* 36, no. 5: 1015–1019.
23 doi:10.1016/j.asr.2005.03.012, 2005.
- 24 Santer, B. D., Sausen, R., Wigley, T. M. L. , Boyle, J. S. , AchutaRao, K., Doutriaux, C.,
25 Hansen, J. E, Meehl, G. A. , Roeckner, E., Ruedy, R., Schmidt, G., Taylor, K. E.: Behavior of
26 tropopause height and atmospheric temperature in models, reanalyses, and observations:
27 Decadal changes, *J. Geophys. Res.*, 108(D1), 4002, doi:10.1029/2002JD002258, 2003.
- 28 [Savage, N. H., Agnew, P., Davis, L. S., Ordonez, C., Thorpe, R., Johnson, C. E., O'Connor,](#)
29 [F. M., and Dalvi, M.: Air quality modelling using the Met Office Unified Model \(AQUM](#)
30 [OS24-26\): model description and initial evaluation, *Geosci. Model Dev.*, 6, 353–372, 2013,](#)
31 [doi:10.5194/gmd-6-353- 2013, 2013.](#)

Formatiert: Schriftart: 12 pt,
Schriftartfarbe: Schwarz

Formatiert: Zeilenabstand: 1,5
Zeilen

1 Schaap, M., Renske, M. A., Timmermans, M. R., Boersen, G. A. C., Builtjes, P. J. H.: The
2 LOTOS–EUROS model: description, validation and latest developments, *Int. J. Environ.*
3 *Pollut.*, 32, No. 2, 270-290, 2008.

4 Schreier, S. F., Richter, A., Kaiser, J. W., and Burrows, J. P.: The empirical relationship
5 between satellite-derived tropospheric NO₂ and fire radiative power and possible implications
6 for fire emission rates of NO_x, *Atmos. Chem. Phys.*, 14, 2447–2466, doi:10.5194/acp-14-
7 2447-2014, 2014.

8 Schultz, M.G., Backman, L., Balkanski, Y., Bjoerndalsaeter, S., Brand, R., Burrows, J.P.,
9 Dalsoeren, S., de Vasconcelos, M., Grodtmann, B., Hauglustaine, D.A., Heil, A.,
10 Hoelzemann, J.J., Isaksen, I.S.A., Kaurola, J., Knorr, W., Ladstaetter-Weißenmayer, B.,
11 Mota, A., Oom, D., Pacyna, J., Panasiuk, D., Pereira, J.M.C., Pulles, T., Pyle, J., Rast, S.,
12 Richter, A., Savage, N., Schnadt, C., Schulz, M., Spessa, A., Staehelin, J., Sundet, J.K.,
13 Szopa, S., Thonicke, K., van het Bolscher M., van Noije, T., van Velthoven, P., Vik, A.F.,
14 Wittrock, F. (2007): REanalysis of the TROpospheric chemical composition over the past 40
15 years (RETRO) — A long-term global modeling study of tropospheric chemistry, Final
16 Report Jülich/ Hamburg, Germany, published as report no. 48/2007 in the series „Reports on
17 Earth System Science“ of the Max Planck Institute for Meteorology, Hamburg, ISSN 1614-
18 1199, 2007.

19 Seinfeld, J. H., and Pandis, S. N.: *Atmospheric Chemistry and Physics: From Air Pollution to*
20 *Climate Change*, John Wiley, Hoboken, N. J., 2006.

21 Selin, N.E., Wu, S., Reilly, J. M., Paltsev, S., Prinn, R.G. and Webster, M.D.: Global health
22 and economic impacts of future ozone pollution. *Environ. Res. Lett.* 4, doi:10.1088/1748-
23 9326/4/4/044014, 2009.

24 [Sheel, V., Sahu, L.K., Kajinu, M., Deushi, M., Stein, O., Nedelec, P.: Seasonal and](#)
25 [interannual variability of carbon monoxide based on MOZAIC observations, MACC](#)
26 [reanalysis, and model simulations over an urban site in India. *J. Geophys. Res.*, 119, 14,](#)
27 [9123–9141, 2014.](#)

28 Shindell, D. T., et al.: Multimodel simulations of carbon monoxide: Comparison with
29 observations and projected near-future changes, *J. Geophys. Res.*, 111, D19306,
30 doi:10.1029/2006JD007100, 2006.

Formatiert: Schriftart: 12 pt.
Schriftartfarbe: Schwarz

Formatiert: Zeilenabstand: 1,5
Zeilen

1 Sinnhuber, B.M., Weber, M., Amankwah, A. and Burrows, J.P.: “Total Ozone during the
2 Unusual Antarctic Winter of 2002.” *Geophysical Research Letters* 30, no. 11, 1580–1584.
3 doi:10.1029/2002GL016798, 2003.

4 Sinnhuber, M., Burrows, J.P., Chipperfield, M., P., Jackman, C. H., Kallenrode, M.-B.,
5 Künzi, K.F., and Quack, M.: A Model Study of the Impact of Magnetic Field Structure on
6 Atmospheric Composition during Solar Proton Events., *Geophys.. Res. Lett.*, 30, 1818–1821,
7 doi:10.1029/2003GL017265, 2003.

8 S. Sitch, S., Cox, P. M., Collins, W. J., Huntingford, C.: Indirect radiative forcing of climate
9 change through ozone effects on the land-carbon sink. *Nature* 448, 791-794,
10 doi:10.1038/nature06059, 2007.

11 Stein, O., Schultz, M. G., Flemming, J., Inness, A., Kaiser, J., Jones, L., Benedetti, A.,
12 Morcrette, J.-J.: MACC Global air quality services – Technical Documentation. MACC
13 project deliverable D_G-RG_3.8, available at:
14 www.gmes-atmosphere.eu/documents/deliverables/g-rg/ (last access: February 2015), 2011.

15 Stein, O., Flemming, J., Inness, A., Kaiser, J. W., and Schultz, M. G.: Global reactive gases
16 and reanalysis in the 5 MACC project, *J. Integr. Environ. Sci.*,
17 doi:10.1080/1943815X.2012.696545, 2012.

18 Stein, O., Huijnen, V., Flemming, J.: Model description of the IFS-MOZART and IFS-TM5
19 coupled systems. MACC-II project deliverable D_55.4, available at:
20 <https://www.gmes-atmosphere.eu/documents/maccii/deliverables/grg/> (last access: February
21 2015), 2013.

22 Stein, O., Schultz, M. G., Bouarar, I., Clark, H., Huijnen, V., Gaudel, A., George, M., and
23 Clerbaux, C.: On the wintertime low bias of Northern Hemisphere carbon monoxide found in
24 10 global model simulations, *Atmos. Chem. Phys.*, 14, 9295–9316, doi:10.5194/acp-14-9295-
25 2014, 2014.

26 Tørseth, K., Aas, W., Breivik, K., Fjæraa, A. M., Fiebig, M., Hjellbrekke, A. G., Lund
27 Myhre, C., Solberg, S., and Yttri, K. E.: Introduction to the European Monitoring and
28 Evaluation Programme (EMEP) and observed atmospheric composition change during
29 1972–2009, *Atmos. Chem. Phys.*, 12, 5447-5481, doi:10.5194/acp-12-5447-2012, 2012.

1 Valcke, S., Redler, R.: OASIS4 User Guide (OASIS4_0_2). PRISM–Support Initiative,
2 Technical Report No 4, available at:
3 http://www.prism.enes.org/Publications/Reports/OASIS4_User_Guide_T4.pdf (last access:
4 February 2015), 2006.

5 Val Martin, M., Heald, C.L., Arnold, S.R.: Coupling dry deposition to vegetation phenology
6 in the Community Earth System Model: Implications for the simulation of surface O₃.
7 *Geophys Res. Lett.*, 41, 2988-2996, doi:10.1002/2014GL059651, 2014.

8 Van der Werf, G. R., Randerson, J. T., Giglio, L., Collatz, G. J., and Kasibhatla, P. S.:
9 Interannual variability in global biomass burning emissions from 1997 to 2004. *Atmos.*
10 *Chem. Phys.*, 6(11):3423–3441, doi:10.5194/acp-6-3423-2006, 2006.

11 Velders, G. J. M., Granier, C., Portmann, R. W., Pfeilsticker, K., Wenig, M., Wagner, T.,
12 Platt, U., Richter, A., and Burrows, J. P.: Global tropospheric NO₂ column distributions:
13 Comparing 3-D model calculations with GOME measurements, *J. Geophys. Res.*, 106,
14 12643–12660, 2001.

15 Wang, P., Stammes, P., van der A, R., Pinardi, G., and van Roozendaal, M.: FRESCO+: An
16 improved O₂ A-band cloud retrieval algorithm for tropospheric trace gas retrievals, *Atmos.*
17 *Chem. Phys.*, 8, 6565-6576, doi:10.5194/acp-8-6565-2008, 2008.

18 Winkler, H., Sinnhuber, M., Notholt, J., Kallenrode, M.B., Steinhilber, F., Vogt, J., Zieger,
19 B., Glassmeier, K.H. and Stadelmann, A.: Modeling impacts of geomagnetic field variations
20 on middle atmospheric ozone responses to solar proton events on long timescales, *J. Geophys.*
21 *Res.* 113, D02302, doi:10.1029/2007JD008574, 2008.

22 WMO:WMO Global Atmosphere Watch (GAW) Strategic Plan: 2008 – 2015. World
23 Meteorological Organization, Geneva, Switzerland, 2007.

24 WMO: Guidelines for the Measurement of Atmospheric Carbon Monoxide, GAW Report No.
25 192, World Meteorological Organization, Geneva, Switzerland, 2010.

26 WMO: WMO/GAW Expert Workshop on Global Long-term Measurements of Nitrogen
27 Oxides and Recommendations for GAW Nitrogen Oxides Network, GAW Report No. 195,
28 World Meteorological Organization, Geneva, Switzerland, 2011.

29

Gelöscht: ¶

1 WMO: 16th WMO/IAEA Meeting on Carbon Dioxide, Other greenhouse Gases and Related
2 Measurement Techniques (GGMT-2011), Geneva, 2012.

3 WMO : Guidelines for the Continuous Measurements of Ozone in the
4 Troposphere, GAW Report No. 209, World Meteorological Organization, Geneva,
5 Switzerland, 2013.

6 Worden, H. M., Deeter, M. N., Edwards, D. P., Gille, J. C., Drummond, J. R. and Nedelec, P.
7 P.: Observations of near-surface carbon monoxide from space using MOPITT multispectral
8 retrievals, *J. Geophys. Res.*, 115, doi:10.1029/2010JD014242, 2010.

9 Worden, H. M., Deeter, M. N., Edwards, D. P., Gille, J., Drummond, J., Emmons, L. K.,
10 Francis, G., Martínez-Alonso, S.: 13 years of MOPITT operations: lessons from MOPITT
11 retrieval algorithm development, *Ann. Geophys.*, 56,, doi:10.4401/ag-6330, 2014.

1 Table 1: List of assimilated data in the MACC_osuite

| Instrument | Satellite | Provider | Version | Type | Status |
|-------------------|------------------|-----------------|----------------|-------------------------------------|---------------------|
| MLS | AURA | NASA | V02 | O ₃ Profiles | 20090901 - 20121231 |
| OMI | AURA | NASA | V883 | O ₃ Total column | 20090901 - 20121231 |
| SBUV-2 | NOAA | NOAA | V8 | O ₃ 6 layer profiles | 20090901 - 20121231 |
| SCIAMACHY | Envisat | KNMI | | O ₃ total column | 20090916 - 20120408 |
| IASI | MetOp-A | LATMOS/ULB | | CO Total column | 20090901 - 20121231 |
| MOPITT | TERRA | NCAR | V4 | CO Total column | 20120705 - 20121231 |
| OMI | AURA | KNMI | DOMINO V2.0 | NO ₂ Tropospheric column | 20120705 - 20121231 |
| OMI | AURA | NASA | v003 | SO ₂ Tropospheric column | 20120705 - 20121231 |
| MODIS | AQUA / TERRA | NASA | Col. 5 | Aerosol total optical depth | 20090901 - 20121231 |

2

1

2 Table 2: Description of the set-up of the MACC_osuite between 9/2009 and 12/2012. Details
3 on the assimilated data are provided in Table 1. A description of the emissions is given in
4 section 2.1.1 in the text.

| Model Cycle | CTM | Assimilated Data | Emissions |
|--------------------|-------------|--|-----------------------------------|
| CY36R1 | MOZART v3.0 | O ₃ (MLS, OMI, SBUV-2 SCIAMACHY), CO (IASI) | RETRO / REAS / GEIA / GFEDv2/GFAS |
| CY37R3 | MOZART v3.5 | O ₃ (MLS, OMI, SBUV-2), CO (IASI, MOPITT), NO ₂ (OMI), SO ₂ (OMI) | MACCcity / MEGAN / GFASv1.0 daily |

5

1 Table 3: List of GAW and EMEP stations used in the evaluation (GAW listed by label, EMEP
 2 listed by region: Northern Europe NE, Central Europe CE and Southern Europe SE).The
 3 numbers behind the name provide the type of gas: 1=O₃, 2=CO, 3=NO₂.

Formatiert: Tiefgestellt

Formatiert: Tiefgestellt

| Station | Label/Region | Programme | Lat | Lon | Alt [m a.s.l.] | Station | Label/Region | Programme | Lat | Lon | Alt [m a.s.l.] |
|--------------------------------|--------------|-----------|--------|---------|----------------|--------------------------------------|--------------|-----------|--------|---------|---------------------------------------|
| Ähtäri I ¹ | NE | EMEP | 62.58 | 24.18 | 180 | Masenberg ¹ | CE | EMEP | 47.35 | 15.88 | Formatiert: Hochgestellt |
| Alert ² | ALT | GAW | 82.45 | -62.52 | 210 | Mauna Loa ¹ | MAU | GAW | 19.54 | -155.58 | Formatiert: Hochgestellt |
| Arrival Heights ¹ | ARH | GAW | -77.80 | 166.67 | 184 | Minamitorishima ^{1,2} | MNM | GAW | 24.29 | 153.98 | Formatiert: Hochgestellt |
| Aspvreten ¹ | NE | EMEP | 58.80 | 17.38 | 20 | Montandon ¹ | CE | EMEP | 47.30 | 6.83 | Formatiert: Hochgestellt |
| Assekrem ¹ | ASS | GAW | 23.27 | 5.63 | 2710 | Monte Cimone ^{1,2} | MCI | GAW | 44.18 | 10.70 | 2165 |
| Aston Hill ¹ | NE | EMEP | 52.50 | -3.03 | 370 | Monte Velho ¹ | SE | EMEP | 38.08 | -8.80 | 43 |
| Auchencortth ¹ | NE | EMEP | 55.79 | -3.24 | 260 | Montelibretti ¹ | CE | EMEP | 42.10 | 12.63 | 48 |
| Ayia Marina ¹ | SE | EMEP | 35.04 | 33.06 | 532 | Montfranc ¹ | CE | EMEP | 45.80 | 2.07 | 810 |
| Barcarola ¹ | SE | EMEP | 38.47 | -6.92 | 393 | Morvan ¹ | CE | EMEP | 47.27 | 4.08 | 620 |
| Baring Head ¹ | BAH | GAW | -41.41 | 174.87 | 85 | Narberth ¹ | NE | EMEP | 51.23 | -4.70 | 160 |
| Barrow ¹ | BAR | GAW | 71.32 | -156.60 | 11 | Neuglobsow ^{1,2} | NGW/NE | GAW/EMEP | 53.17 | 13.03 | 62 |
| BEO Moussala ^{1,2} | BEO | GAW | 42.18 | 23.59 | 2925 | Neumayer ¹ | NEU | GAW | -70.65 | -8.25 | 42 |
| Birkenes ¹ | NE | EMEP | 58.38 | 8.25 | 190 | Niembro ¹ | CE | EMEP | 43.44 | -4.85 | 134 |
| Bredkälén ¹ | NE | EMEP | 63.85 | 15.33 | 404 | Norra-Kvill ¹ | NE | EMEP | 57.81 | 15.56 | 261 |
| Bush ¹ | NE | EMEP | 55.86 | -3.21 | 180 | O Saviñao ¹ | CE | EMEP | 43.23 | -7.70 | 506 |
| Cabauw ¹ | NE | EMEP | 51.97 | 4.92 | 60 | Offagne ¹ | CE | EMEP | 49.88 | 5.20 | 430 |
| Cabo de Crêpus ¹ | CE | EMEP | 42.32 | 3.32 | 23 | Oulanka ¹ | NE | EMEP | 66.32 | 29.40 | 310 |
| Cairo ¹ | CAI | GAW | 30.08 | 31.28 | 35 | Pallas ¹ | NE | EMEP | 68.00 | 24.15 | 340 |
| Campisabalps ¹ | CE | EMEP | 41.28 | -3.14 | 1360 | Payerne ^{1,2} | PAY/CE | GAW/EMEP | 46.81 | 6.94 | 510 |
| Cape Grim ¹ | CAG | GAW | -40.68 | 144.68 | 94 | Penausende ¹ | CE | EMEP | 41.28 | -5.86 | 985 |
| Cape Point ^{1,2} | CAP | GAW | -34.35 | 18.48 | 230 | Peyrusse Vieille ¹ | CE | EMEP | 43.62 | 0.18 | 200 |
| Cape Verde ^{1,2} | CVO | GAW | 16.85 | -24.87 | 10 | Pic du Midi ^{1,2} | PIC/CE | GAW/EMEP | 42.94 | 0.14 | 2877 |
| Charlton Mackrell ¹ | NE | EMEP | 51.06 | -2.68 | 54 | Pillersdor ¹ | CE | EMEP | 48.72 | 15.94 | 315 |
| Chaumont ¹ | CE | EMEP | 47.05 | 6.98 | 1130 | Preila ¹ | NE | EMEP | 55.35 | 21.07 | Formatiert: Hochgestellt |
| Chibougamaü ² | CHI | GAW | 49.68 | -74.34 | 393 | Prestebakke ¹ | NE | EMEP | 59.00 | 11.53 | 160 |
| Chopok ¹ | CE | EMEP | 48.93 | 19.58 | 2008 | Puy de Dôme ^{1,2} | PUY/CE | GAW/EMEP | 45.77 | 2.95 | 1465 |
| Concordia ¹ | CON | GAW | -75.10 | 123.33 | 3233 | Ragged Point ¹ | RAG | GAW | 13.17 | -59.43 | 45 |
| De Zilk ¹ | NE | EMEP | 52.30 | 4.50 | 4 | Rao ¹ | NE | EMEP | 57.39 | 11.91 | 10 |
| Diabla Gora ¹ | NE | EMEP | 54.15 | 22.07 | 157 | Revin ¹ | CE | EMEP | 49.90 | 4.63 | 390 |
| Dobele ¹ | DOB | GAW | 56.37 | 23.19 | 42 | Rigi ^{1,2,3} | RIG/CE | GAW/EMEP | 47.07 | 8.46 | 1030 |
| Doñana ¹ | SE | EMEP | 37.03 | -6.33 | 5 | Rojen Peak ¹ | CE | EMEP | 41.70 | 24.74 | 1750 |
| Donon ¹ | CE | EMEP | 48.50 | 7.13 | 775 | Rucava ¹ | RUC/NE | GAW/EMEP | 56.10 | 21.10 | 18 |
| Dunkelsteinerwald ¹ | CE | EMEP | 48.37 | 15.55 | 320 | Ryorj ^{1,2} | RYO | GAW | 39.03 | 141.82 | Formatiert: Hochgestellt |
| East Trout Lake ² | ETL | GAW | 54.35 | -104.98 | 492 | Sable Island ² | SAB | GAW | 43.93 | -60.02 | Formatiert: Hochgestellt |
| Egbert ² | EGB | GAW | 44.23 | -79.78 | 253 | San Pablo de los Montes ¹ | SE | EMEP | 39.55 | -4.35 | Formatiert: Englisch (Großbritannien) |
| Eibergen ¹ | NE | EMEP | 52.08 | 6.57 | 20 | Sandve ¹ | NE | EMEP | 59.20 | 5.20 | |
| Els Torms ¹ | CE | EMEP | 41.40 | 0.72 | 470 | Schauinsland ^{1,2,3} | SCH/CE | GAW/EMEP | 47.92 | 7.92 | 1205 |
| Eskdalemuir ¹ | NE | EMEP | 55.31 | -3.20 | 243 | Schmücke ¹ | NE | EMEP | 50.65 | 10.77 | 937 |
| Esrang ¹ | NE | EMEP | 67.88 | 21.07 | 475 | Sibton ¹ | NE | EMEP | 52.29 | 1.46 | 46 |

| | | | | | | | | | | | |
|-----------------------------------|--------|----------|--------|---------|------|--------------------------------|--------|----------|--------|---------|------|
| Estevan Poicht ^{1,2} | ESP | GAW | 49.38 | -126.55 | 39 | Śnieżka ¹ | NE | EMEP | 50.73 | 15.73 | 1603 |
| Eupen ¹ | NE | EMEP | 51.46 | 6.00 | 295 | Sonnblick ^{1,2,3} | SBL/CE | GAW/EMEP | 47.05 | 12.96 | 3106 |
| Everest - Pyramid ¹ | EVP | GAW | 27.96 | 86.82 | 5079 | South Pole ¹ | SPO | GAW | -89.98 | -24.80 | 2810 |
| Finokalia ¹ | SE | EMEP | 35.32 | 25.67 | 250 | Spitsbergen ¹ | NE | EMEP | 78.90 | 11.88 | 474 |
| Forsthoft ¹ | CE | EMEP | 48.10 | 15.91 | 581 | St. Osyth ¹ | NE | EMEP | 51.78 | 1.08 | 8 |
| Fraserdale ² | FRA | GAW | 49.88 | -81.57 | 210 | Stará Lesná ¹ | CE | EMEP | 49.15 | 20.28 | 808 |
| Gänserndorf ¹ | CE | EMEP | 48.33 | 16.73 | 161 | Starina ¹ | CE | EMEP | 49.05 | 22.27 | 345 |
| Gerlitz ¹ | CE | EMEP | 46.69 | 13.92 | 1895 | Stixneusiedl ¹ | CE | EMEP | 48.05 | 16.68 | 240 |
| Graz Platte ¹ | CE | EMEP | 47.11 | 15.47 | 651 | Strath Vaich Dam ¹ | NE | EMEP | 57.73 | -4.77 | 270 |
| Great Dun Fell ¹ | NE | EMEP | 54.68 | -2.45 | 847 | Summit ¹ | SUM | GAW | 72.58 | -38.48 | 3238 |
| Grebzen ¹ | CE | EMEP | 47.04 | 14.33 | 1648 | Svratouch ¹ | CE | EMEP | 49.73 | 16.05 | 737 |
| Grimsoe ¹ | NE | EMEP | 59.73 | 15.47 | 132 | Syowa Station ¹ | SYO | GAW | -69.00 | 39.58 | 16 |
| Harwell ¹ | NE | EMEP | 51.57 | -1.32 | 137 | Tänikon ¹ | CE | EMEP | 47.48 | 8.90 | 540 |
| Haunsberg ¹ | CE | EMEP | 47.97 | 13.02 | 730 | Topolniky ¹ | CE | EMEP | 47.96 | 17.86 | 113 |
| Heidenreichstein ¹ | CE | EMEP | 48.88 | 15.05 | 570 | Trinidad Head ¹ | TRI | GAW | 41.05 | -124.15 | 120 |
| High Muffles ¹ | NE | EMEP | 54.33 | -0.80 | 267 | Tsukuba ¹ | TSU | GAW | 36.05 | 140.13 | 25 |
| Hurdal ¹ | NE | EMEP | 60.37 | 11.08 | 300 | Tudor Hill ¹ | TUD | GAW | 32.27 | -64.87 | 30 |
| Illmitz ¹ | CE | EMEP | 47.77 | 16.77 | 117 | Tustervatn ¹ | NE | EMEP | 65.83 | 13.92 | 439 |
| Iskrba ¹ | ISK/CE | GAW/EMEP | 45.56 | 14.86 | 520 | Tutuila ¹ | TUT | GAW | -14.24 | -170.57 | 42 |
| Izaña (Tenerife) ^{1,2} | IZO | GAW | 28.30 | -16.50 | 2367 | Ushuaia ^{1,2} | USH | GAW | -54.85 | -68.32 | 18 |
| Jarczew ¹ | NE | EMEP | 51.82 | 21.98 | 180 | Utö ¹ | NE | EMEP | 59.78 | 21.38 | 7 |
| Jungfrauoch ^{1,2,3} | JFJ/CE | GAW/EMEP | 46.55 | 7.99 | 3578 | Vavihill ¹ | NE | EMEP | 56.01 | 13.15 | 175 |
| Karaszok ¹ | NE | EMEP | 69.47 | 25.22 | 333 | Vezin ¹ | NE | EMEP | 50.50 | 4.99 | 160 |
| Keldsno ¹ | NE | EMEP | 54.73 | 10.73 | 10 | Vilsandl ¹ | NE | EMEP | 58.38 | 21.82 | 6 |
| Kollumerwaard ^{1,2,3} | KOW/NE | GAW/EMEP | 53.33 | 6.28 | 1 | Vindeln ¹ | VIN/NE | GAW/EMEP | 64.25 | 19.77 | 225 |
| Košetice ^{1,2,3} | KOS/CE | GAW/EMEP | 49.58 | 15.08 | 534 | Virolahti II ¹ | NE | EMEP | 60.53 | 27.69 | 4 |
| Kovk ¹ | KOV/CE | GAW/EMEP | 46.12 | 15.11 | 600 | Vorhegg ¹ | CE | EMEP | 46.68 | 12.97 | 1020 |
| K-puszta ¹ | CE | EMEP | 46.97 | 19.58 | 125 | Vredepeel ¹ | NE | EMEP | 51.54 | 5.85 | 28 |
| Krvavec ^{1,2} | KRV/CE | GAW/EMEP | 46.30 | 14.54 | 1740 | Waldhof ¹ | WAL/NE | GAW/EMEP | 52.80 | 10.77 | 8 |
| La Coulonche ¹ | CE | EMEP | 48.63 | -0.45 | 309 | Westerland ¹ | WES/NE | GAW/EMEP | 54.93 | 8.32 | 8 |
| La Tardière ¹ | CE | EMEP | 46.65 | -0.75 | 143 | Weybourne ¹ | NE | EMEP | 52.95 | 1.12 | 8 |
| Lac La Biche ^{1,2} | LAC | GAW | 54.95 | -112.45 | 540 | Wicken Fen ¹ | NE | EMEP | 52.30 | -0.29 | 8 |
| Ladybower Res. ¹ | NE | EMEP | 53.40 | -1.75 | 420 | Yarner Wood ¹ | NE | EMEP | 50.59 | -3.71 | 119 |
| Lahemaa ¹ | NE | EMEP | 59.50 | 25.90 | 32 | Yonagunijima ^{1,2} | YON | GAW | 24.47 | 123.02 | 30 |
| Lauder ¹ | LAU | GAW | -45.03 | 169.67 | 370 | Zarodnje ¹ | CE | EMEP | 46.42 | 15.00 | 770 |
| Le Casset ¹ | CE | EMEP | 45.00 | 6.47 | 750 | Zarra ¹ | SE | EMEP | 39.09 | -1.10 | 885 |
| Leba ¹ | NE | EMEP | 54.75 | 17.53 | 2 | Zavodnje ¹ | ZAV | GAW | 46.43 | 15.00 | 770 |
| Lerwick ¹ | NE | EMEP | 60.13 | -1.18 | 85 | Zillertaler Alpen ¹ | CE | EMEP | 47.14 | 11.87 | 1970 |
| Lille Valby ¹ | NE | EMEP | 55.69 | 12.13 | 10 | Zingst ¹ | ZIN/NE | GAW/EMEP | 54.43 | 12.73 | 1 |
| Lough Nava ¹ | NE | EMEP | 54.44 | -7.87 | 126 | Zoebelboden ¹ | CE | EMEP | 47.83 | 14.44 | 899 |
| Lullington Heath ¹ | NE | EMEP | 50.79 | 0.17 | 120 | Zosen ¹ | ZOS/NE | GAW/EMEP | 57.13 | 25.90 | 8 |
| Mace Head ¹ | NE | EMEP | 53.17 | -9.50 | 15 | Zugspitze ^{1,2} | SFH | GAW | 47.42 | 10.98 | 2656 |
| Market Harborough ¹ | NE | EMEP | 52.55 | -0.77 | 145 | | | | | | |

Formatiert: Schriftart: Nicht Fett

Gelöscht: EMEP

Formatiert: Hochgestellt

Gelöscht:

1

2

1 Table 4: Modified normalized mean bias (MNMB) [%], correlation coefficient (R), and root
 2 mean square error (RMSE) [ppb] derived from the evaluation of the MACC_osuite with
 3 Global Atmosphere Watch (GAW) O₃ surface observations during the period 09/2009 to
 4 12/2012.

| Station | ARH | ASS | BAH | BAR | BEO | CAI | CAG | CAP | CVO | CON | DOB | EVP | ISK | IZO | JFJ | KOW | KOS |
|-------------|-------|------|------|-------|-------|------|-------|------|------|-------|------|------|------|------|-----|------|------|
| MNMB | -39.8 | -6.3 | -8.6 | -35.1 | -21.4 | 70.1 | -12.7 | 13.7 | 15.2 | -81.6 | 6.3 | 18.4 | 67.2 | 10.4 | 1.9 | 5.8 | -5.9 |
| R | 0.6 | 0.7 | 0.5 | 0.3 | 0.4 | -0.1 | 0.4 | 0.6 | 0.6 | 0.3 | 0.3 | 0.7 | 0.1 | 0.5 | 0.7 | 0.6 | 0.6 |
| RMSE | 10.6 | 6.5 | 8.0 | 13.8 | 20.4 | 29.2 | 8.9 | 7.6 | 8.0 | 17.2 | 14.3 | 12.0 | 34.5 | 10.8 | 7.4 | 12.0 | 16.3 |

5

| Station | KOV | KRV | LAU | MAU | MNM | MCI | NGW | NEU | PAY | PIC | PUY | RAG | RIG | RUC | RYO | SCH | SBL |
|-------------|------|------|------|------|------|-----|-------|-------|-------|-----|------|------|-------|------|------|------|-----|
| MNMB | 21.2 | 9.5 | -5.5 | 13.7 | 38.6 | 2.3 | -11.4 | -45.2 | -28.8 | 5.5 | 12.8 | 38.6 | -80.3 | -0.1 | 10.5 | 8.5 | 8.1 |
| R | 0.6 | 0.6 | 0.5 | 0.6 | 0.8 | 0.7 | 0.5 | 0.5 | 0.7 | 0.6 | 0.6 | 0.6 | 0.3 | 0.3 | 0.1 | 0.7 | 0.6 |
| RMSE | 19.5 | 11.1 | 9.0 | 11.5 | 13.0 | 8.2 | 14.3 | 11.4 | 15.6 | 7.7 | 10.6 | 10.6 | 28.4 | 15.0 | 14.4 | 12.2 | 9.3 |

6

| Station | SFH | SPO | SUM | SYO | TRI | TSU | TUD | TUT | USH | VIN | WAL | WES | YON | ZAV | ZIN | ZOS |
|-------------|------|-------|-------|-------|------|------|------|------|------|------|-------|-------|------|------|-------|------|
| MNMB | 10.1 | -70.6 | -24.4 | -31.2 | 3.2 | 55.1 | 45.3 | 40.2 | -7.0 | 4.6 | -18.0 | -12.3 | 22.0 | 19.7 | -17.5 | 22.3 |
| R | 0.6 | 0.4 | 0.5 | 0.7 | 0.3 | 0.0 | 0.5 | 0.8 | 0.5 | 0.4 | 0.6 | 0.6 | 0.7 | 0.6 | 0.4 | 0.2 |
| RMSE | 9.3 | 16.3 | 11.7 | 8.9 | 13.3 | 27.6 | 18.2 | 8.0 | 7.6 | 11.2 | 13.6 | 11.6 | 13.6 | 18.6 | 13.9 | 17.0 |

7

1 Table 5: Modified normalized mean bias (MNMB) [%], correlation coefficient (R), and root
 2 mean square error (RMSE) [ppb] derived from the evaluation of the MACC_osuite with
 3 Global Atmospheric Watch (GAW) CO surface observations during the period 09/2009 to
 4 12/2012.

| Station | ALT | BEO | CAP | CHI | CVO | EGB | ESP | ETL | FRA | IZO | JFJ | KOS | KOW | KRV | LAC | MCI | MNM |
|-------------|------|-------|------|------|------|------|------|-------|-------|------|-------|-------|------|-------|-------|-------|------|
| MNMB | -6.9 | -36.1 | 29.7 | -7.3 | -0.6 | 4.5 | -1.7 | -19.9 | -12.0 | -6.8 | -15.1 | -50.1 | -5.9 | -30.4 | -24.2 | -19.0 | 6.4 |
| R | 0.5 | 0.0 | 0.6 | 0.4 | 0.7 | 0.3 | 0.5 | 0.1 | 0.3 | 0.7 | 0.6 | 0.2 | 0.4 | 0.4 | 0.0 | 0.6 | 0.8 |
| RMSE | 23.4 | 90.3 | 20.4 | 31.1 | 14.2 | 60.1 | 25.7 | 53.9 | 35.9 | 15.3 | 25.8 | 131.1 | 70.1 | 49.1 | 58.5 | 32.0 | 22.0 |

5

| Station | NGW | PAY | PIC | PUY | RIG | RYO | SAB | SBL | SCH | SFH | USH | YON |
|-------------|------|------|------|-------|-------|------|------|-------|-------|-------|------|------|
| MNMB | -1.7 | -7.3 | -9.3 | -10.4 | 28.2 | -4.8 | -8.1 | -25.1 | -15.8 | -25.7 | -9.1 | -1.6 |
| R | 0.4 | 0.3 | 0.7 | 0.6 | 0.0 | 0.4 | 0.4 | 0.5 | 0.5 | 0.4 | 0.6 | 0.7 |
| RMSE | 61.6 | 99.2 | 18.4 | 30.6 | 143.5 | 44.5 | 31.6 | 36.8 | 39.8 | 45.0 | 12.3 | 62.3 |

6

1 Table 6: Modified normalized mean bias (MNMB) [%] derived from CO satellite
2 observations (MOPITT) and the MACC_osuite simulations of CO total columns from
3 10/2009 until 06/2012 averaged over different regions.

| | Oct 09 | Nov 09 | Dec 09 | Jan 10 | Feb 10 | Mar 10 | Apr 10 | May 10 | Jun 10 | Jul 10 | Aug 10 |
|------------------|--------|--------|--------|--------|--------|--------|--------|--------|--------|--------|--------|
| Europe | 4.17 | 1.35 | -7.02 | -7.17 | -7.84 | -8.56 | -5.20 | -2.15 | -2.96 | 0.75 | -2.88 |
| Alaska | 0.31 | -3.16 | -6.71 | -8.85 | -6.39 | -3.13 | -4.49 | -3.85 | -8.69 | -6.18 | -3.94 |
| Siberia | 2.02 | 1.62 | -1.44 | -2.75 | -1.36 | -2.27 | -3.58 | -2.93 | -5.30 | 4.21 | -8.43 |
| N. Africa | 6.53 | 9.17 | 5.82 | 7.05 | 3.45 | -2.96 | -3.53 | -1.75 | -3.40 | -1.21 | -3.58 |
| S. Africa | -12.45 | -9.44 | 3.10 | 6.53 | 8.27 | 6.63 | 3.57 | 2.33 | 7.34 | 0.57 | -2.75 |
| S. Asia | 9.20 | 13.73 | 6.95 | 6.41 | 6.69 | 1.12 | 3.18 | 1.26 | -3.01 | 1.98 | 2.15 |
| E. Asia | 8.04 | 12.33 | -5.86 | -9.18 | -6.64 | -4.49 | -5.12 | -5.61 | -7.72 | -4.34 | -2.80 |
| US | 9.73 | 6.71 | -5.42 | -7.75 | -10.88 | -6.26 | -3.80 | -2.04 | 1.58 | 2.54 | 2.98 |
| | Sep 10 | Oct 10 | Nov 10 | Dec 10 | Jan 11 | Feb 11 | Mar 11 | Apr 11 | May 11 | Jun 11 | Jul 11 |
| Europe | -1.97 | -0.92 | -2.94 | -7.78 | -15.41 | -17.22 | -18.78 | -17.34 | -13.34 | -6.62 | -3.91 |
| Alaska | -5.00 | -1.89 | -4.87 | -7.51 | -14.54 | -9.90 | -9.29 | -12.54 | -11.95 | -10.04 | -4.73 |
| Siberia | -2.94 | -1.93 | -1.73 | -3.02 | -7.71 | -7.78 | -12.09 | -21.99 | -17.23 | -11.59 | -4.97 |
| N. Africa | -1.22 | 3.33 | 5.98 | 7.03 | -0.53 | 4.31 | 2.66 | 1.37 | 4.23 | 4.71 | 4.37 |
| S. Africa | -5.13 | 2.84 | 7.39 | 4.37 | 1.41 | 3.39 | 3.80 | 0.99 | 5.71 | 3.45 | -2.75 |
| S. Asia | 5.05 | 6.72 | 9.63 | 10.30 | 2.19 | 2.91 | 1.48 | -1.76 | 1.68 | 1.62 | 2.90 |
| E. Asia | 6.13 | 6.93 | 2.44 | 3.23 | -11.25 | -9.18 | -9.63 | -8.58 | -4.73 | -1.62 | 5.00 |
| US | 0.08 | -0.71 | 1.20 | -8.06 | -18.30 | -16.98 | -14.33 | -13.52 | -8.10 | -4.72 | -0.64 |
| | Aug 11 | Sep 11 | Oct 11 | Nov 11 | Dec 11 | Jan 12 | Feb 12 | Mar 12 | Apr 12 | May 12 | Jun 12 |
| Europe | -2.57 | -7.28 | -10.80 | -11.85 | -14.79 | -13.50 | -14.16 | -15.30 | -11.49 | -7.00 | -3.65 |
| Alaska | -5.69 | -11.86 | -18.05 | -14.33 | -12.29 | -11.50 | -11.24 | -11.92 | -9.42 | -8.71 | -4.74 |
| Siberia | -6.05 | -15.16 | -16.50 | -10.32 | -11.59 | -10.15 | -8.45 | -13.14 | -12.18 | -11.08 | -4.45 |
| N. Africa | 6.15 | 5.35 | 6.27 | -0.93 | 3.37 | 2.04 | 1.11 | -5.90 | -3.40 | -3.59 | -0.95 |
| S. Africa | -6.70 | -4.43 | -0.58 | 3.64 | 4.66 | 4.25 | 2.91 | 0.91 | 3.41 | 1.33 | -1.23 |
| S. Asia | 3.80 | 2.27 | 4.24 | 4.76 | 7.00 | 3.24 | 1.72 | -1.23 | -0.90 | 0.49 | -0.61 |
| E. Asia | 3.05 | 1.60 | -2.60 | -2.48 | -5.15 | -5.56 | -4.63 | -0.85 | -0.36 | -2.63 | 0.68 |
| US | -1.17 | -2.40 | -4.23 | -6.14 | -10.84 | -13.30 | -14.87 | -9.19 | -6.94 | -2.88 | -2.55 |

4

1 Table 7: Statistics derived from satellite observations (SCIAMACHY from 09/2009 until
 2 03/2012, GOME-2 from 04/2012 to 12/2012) and the MACC_osuite simulations of daily
 3 tropospheric NO₂ VCD [10^{15} molec cm⁻²] averaged over different regions for September 2009
 4 to December 2012.

| Region | United States | Europe | South Asia | East Asia | South Africa | North Africa |
|---|---------------|--------|------------|-----------|--------------|--------------|
| Model mean NO ₂ VCD [10^{15} molec cm ²] | 2.6 | 2.1 | 1.0 | 2.4 | 0.8 | 0.9 |
| Satellite mean NO ₂ VCD [10^{15} molec cm ²] | 3.1 | 3.6 | 1.2 | 6.2 | 1.1 | 0.9 |
| Modified normalized mean bias (MNMB) [%] | -17.3 | -49.0 | -13.4 | -70.7 | -36.8 | -0.4 |
| Root mean square error (RMSE) [10^{15} molec cm ²] | 1.2 | 2.0 | 0.3 | 6.0 | 0.5 | 0.3 |
| Correlation coefficient (R) [dimensionless] | 0.6 | 0.8 | 0.8 | 0.8 | 0.6 | 0.5 |

5

1 Table 8: Modified normalized mean bias (MNMB) [%], correlation coefficient (R), and root
2 mean square error (RMSE) [ppb] derived from the evaluation of the MACC_osuite with
3 Global Atmospheric Watch (GAW) NO₂ surface observations during the period 09/2009 to
4 12/2012.

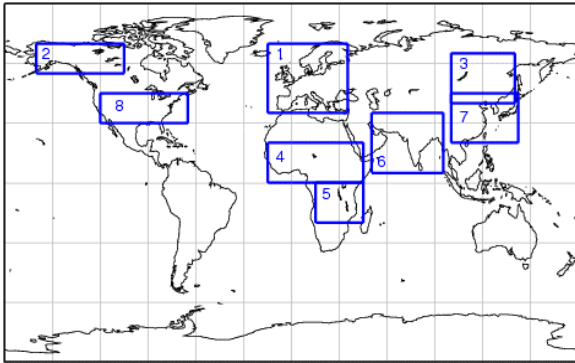
Formatiert: Schriftart: Times
New Roman, 12 pt,
Schriftartfarbe: Schwarz,
Englisch (Großbritannien)

Formatiert: Tiefgestellt

Formatiert: Schriftart: Times
New Roman, 12 pt,
Schriftartfarbe: Schwarz,
Englisch (Großbritannien)

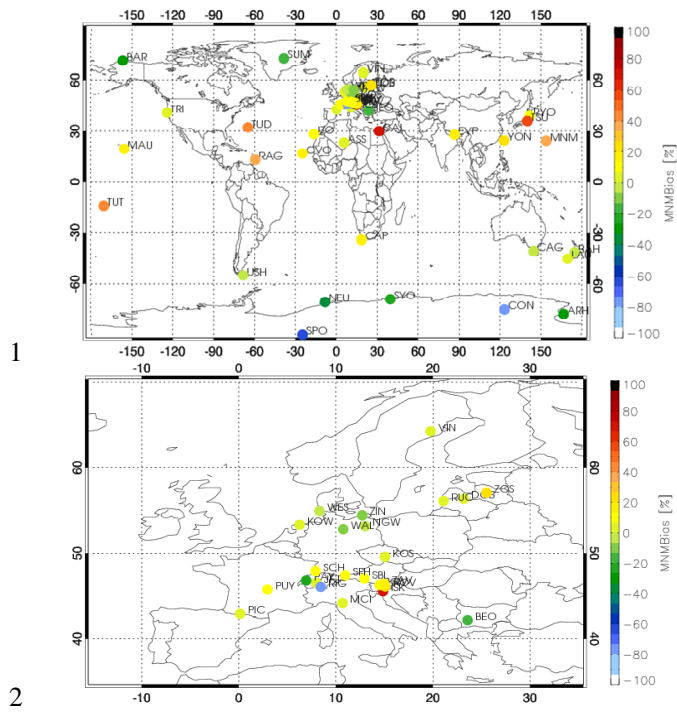
| Station | JFJ | KOW | KOS | RIG | SCH | SBL |
|----------------|------------|------------|------------|------------|------------|------------|
| MNMB | -44.7 | -28.7 | -38.5 | 68.0 | -25.7 | -160.6 |
| R | 0.2 | 0.6 | 0.4 | 0.2 | 0.4 | 0.1 |
| RMSE | 0.3 | 5.2 | 5.4 | 8.9 | 2.2 | 0.9 |

1



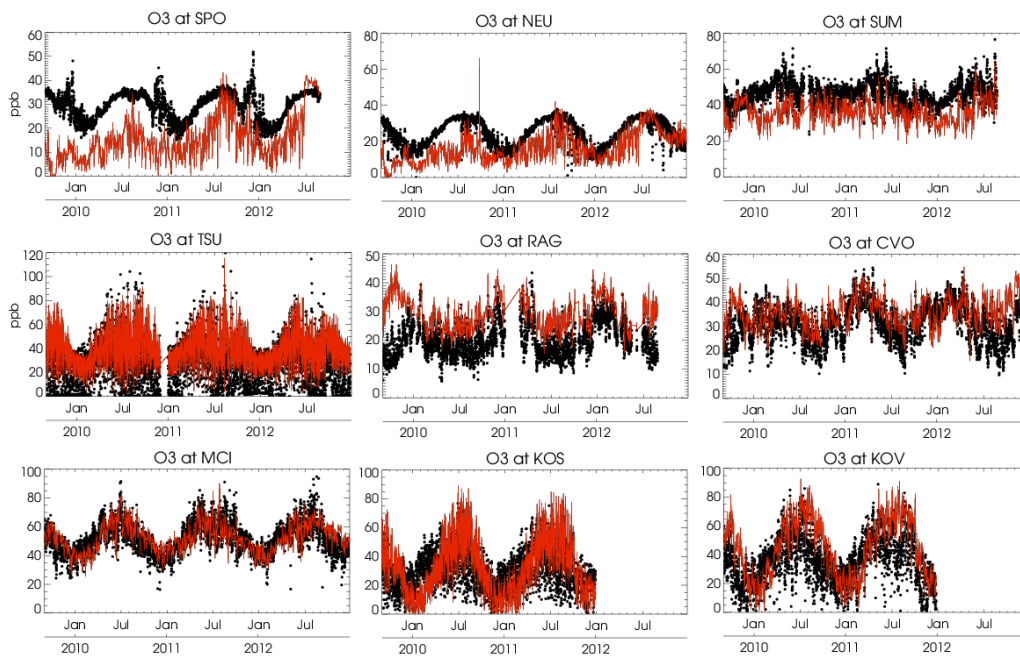
2

3 Figure 1: Regions used for regional data-stratification in the troposphere for the comparison
4 with satellite data. The following regions are defined: **1** Europe (15W– 35E, 35N–70N), **2**
5 Alaska (150W–105W, 55N–70N), **3** Siberia (100E–140E, 40N–65N), **4** North Africa (15W–
6 45E, 0N–20N), **5** South Africa (15E–45E, 20S–0S), **6** South Asia (50E–95E, 5N–35N), **7** East
7 Asia (100E–142E, 20N–45N), **8** United States (120W–65W, 30N–45N).



3 Figure 2: Modified normalized mean biases (MNMBs) [%] derived from the evaluation of the
 4 MACC_osuite with GAW O₃ surface observations during the period 09/2009 to 12/2012
 5 globally (top), and for Europe (bottom). Blue colours represent large negative values;
 6 red/brown colours represent large positive values.

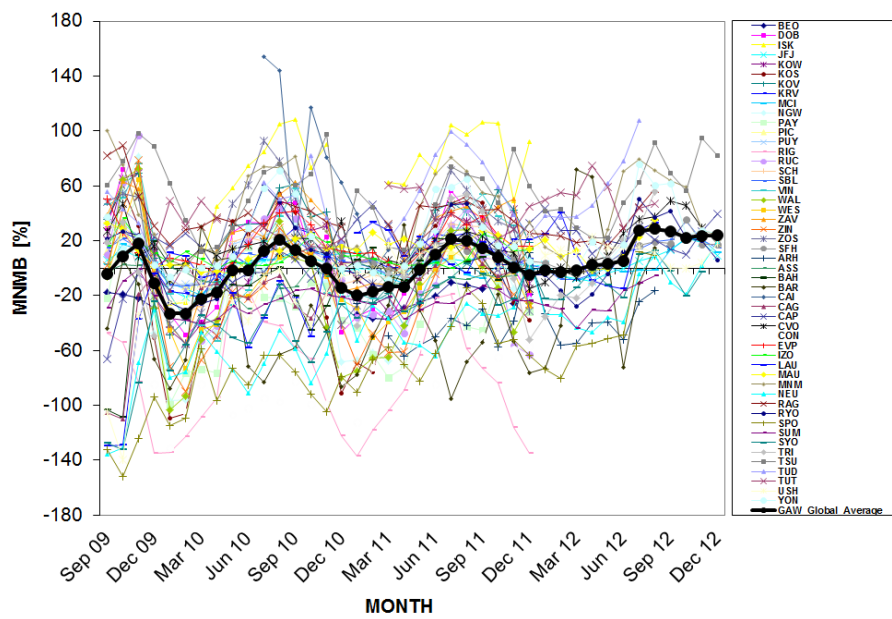
Gelöscht: below



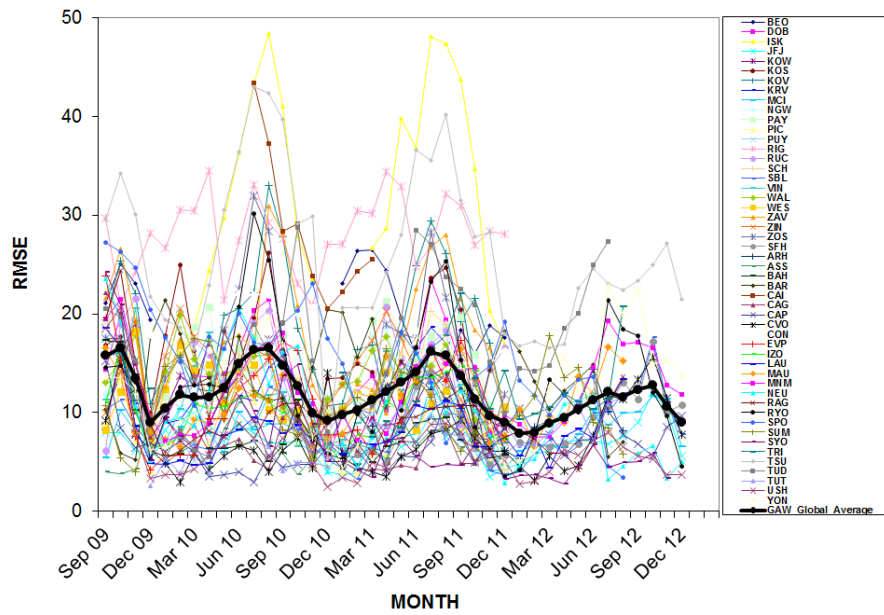
1

2 Figure 3: Time series plots of the MACC_osuite 6-hourly O₃ mixing ratios (red) and GAW
 3 surface observations (black) for South Pole-SPO (Antarctica), Neumayer-NEU (Antarctica),
 4 Summit-SUM (Denmark), Tsukuba-TSU (Japan), Ragged Point-RAG, (Barbados), Cape
 5 Verde Observatory-CVO (Cape Verde), Monte Cimone-MCI (Italy), Kosetice-KOS (Czech
 6 Republic), and Kovk- KOV(Slovenia) during the period 09/2009 to 12/2012. Unit: ppb

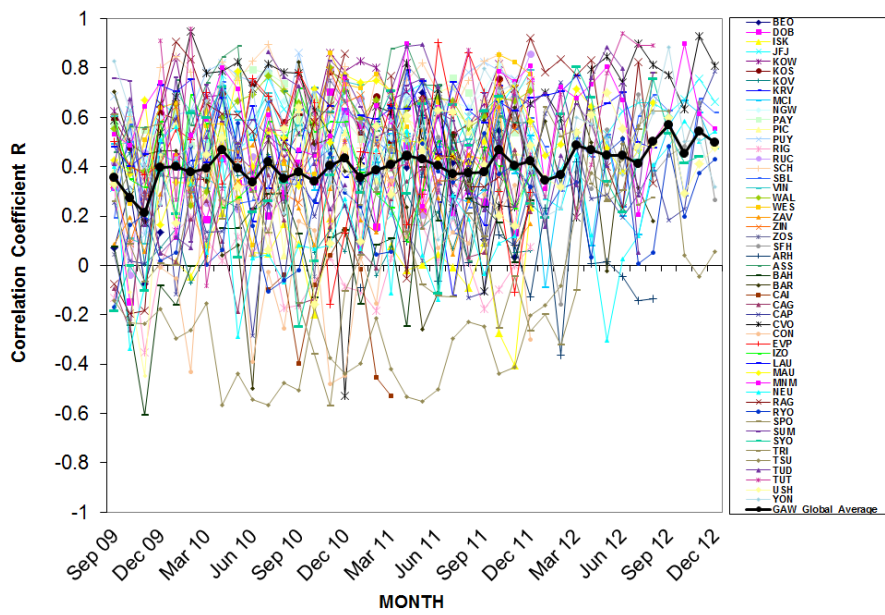
Gelöscht: ,



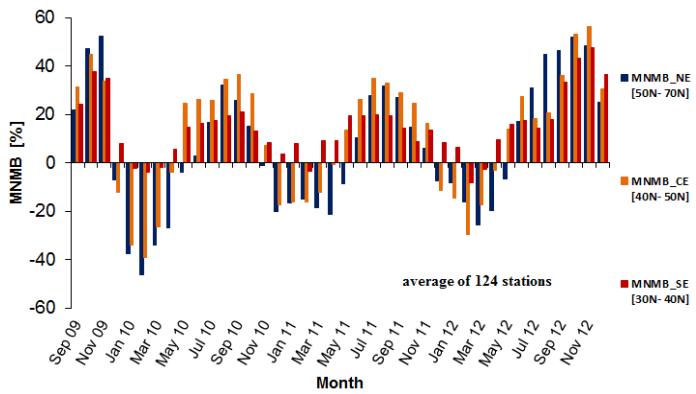
1
 2 Figure 4: Modified normalized mean bias (MNMB) in % derived from the evaluation of the
 3 MACC_osuite with GAW O₃ surface observations during the period September 2009 to
 4 December 2012 (black line: global average of 50 GAW stations. Multi-coloured lines:
 5 individual station results, see legend to the right).



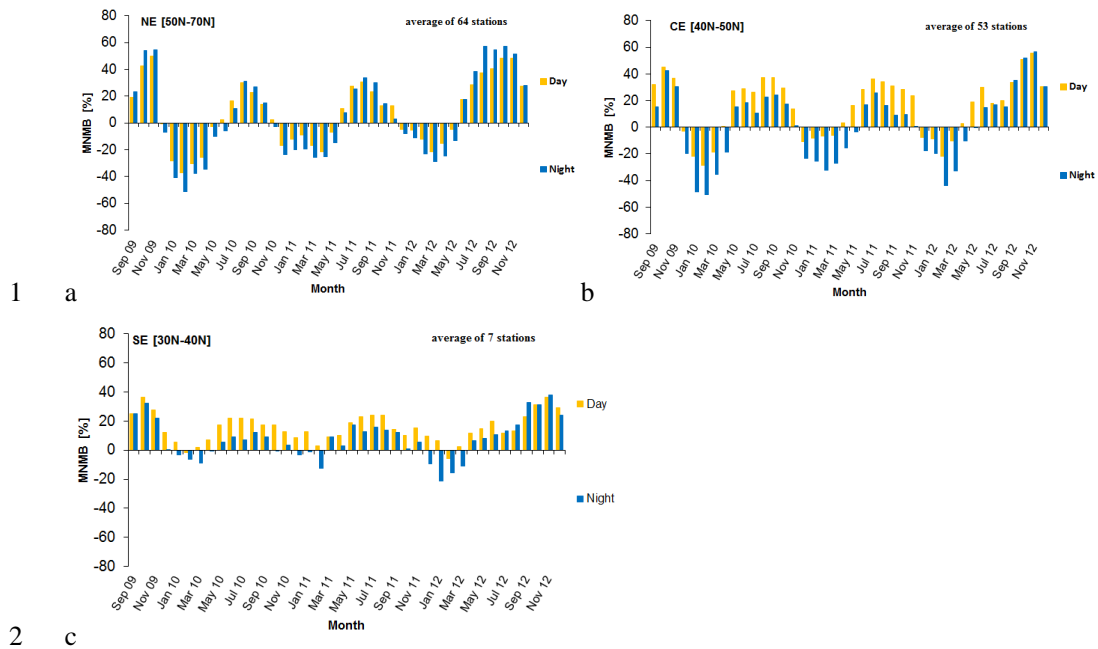
1
 2 Figure 5: Root mean square error (RMSE) in ppb derived from the evaluation of the
 3 MACC_osuite with GAW O₃ surface observations during the period September 2009 to
 4 December 2012 (black line: global average of 50 GAW stations. Multi-coloured lines:
 5 individual station results, see legend to the right).



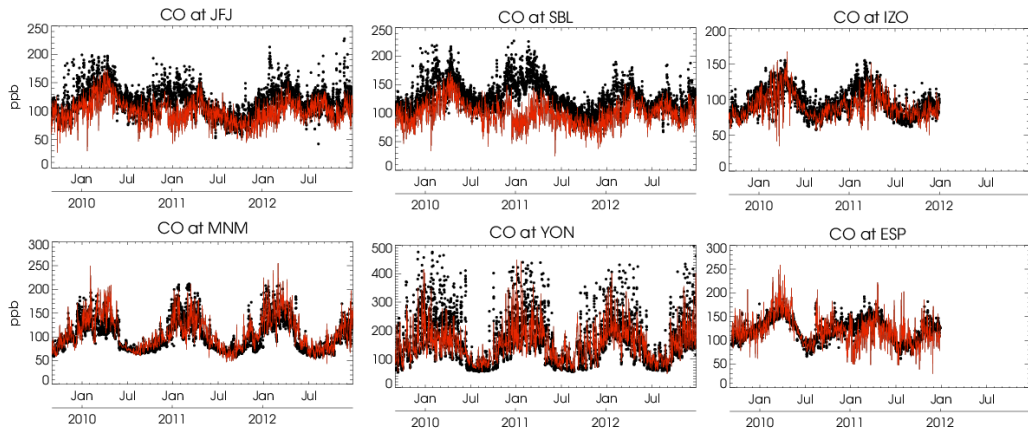
1
 2 Figure 6: Correlation coefficient (R), derived from the evaluation of the MACC_osuite with
 3 GAW O₃ surface observations during the period September 2009 to December 2012 (black
 4 line: global average of 50 GAW stations. Multi-coloured lines: individual station results, see
 5 legend to the right).



1
 2 Figure 7: Modified normalized mean biases (MNMBs) derived from the evaluation of the
 3 MACC_osuite with EMEP O₃ surface observations in three different parts in Europe (blue:
 4 Northern Europe, orange: Central Europe, red: Southern Europe) during the period September
 5 2009 to December 2012.



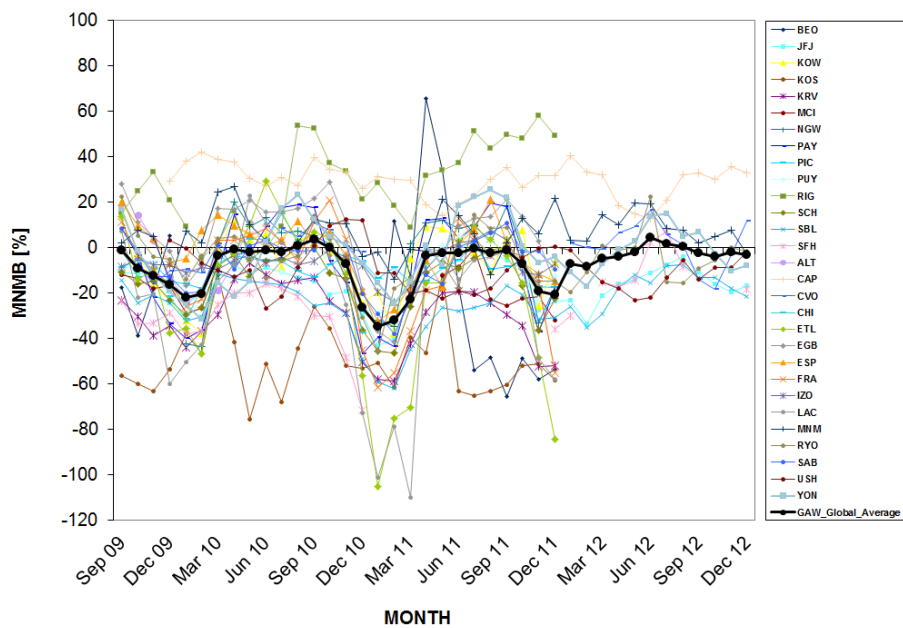
3 Figure 8: Modified normalized mean biases (MNMBs) derived from the evaluation of the
 4 MACC_osuite with EMEP O₃ surface observations during day-time (yellow color), and night-
 5 time (blue color) over northern Europe (a), central Europe (b) and southern Europe (c) during
 6 the period September 2009 to December 2012.



1
 2 Figure 9: Time series plots of the MACC_osuite 6-hourly CO mixing ratios (red) and GAW
 3 surface observations (black) for Jungfraujoch- JFJ (Switzerland), Sonnblick- SBL (Austria),
 4 Izana Observatory- IZO (Tenerife), Minamitorishima- MNM (Japan), Yonagunijima- YON
 5 (Japan) and Estevan Point- EVP (Canada) during the period 09/2009 to 12/2012. Unit: ppb.

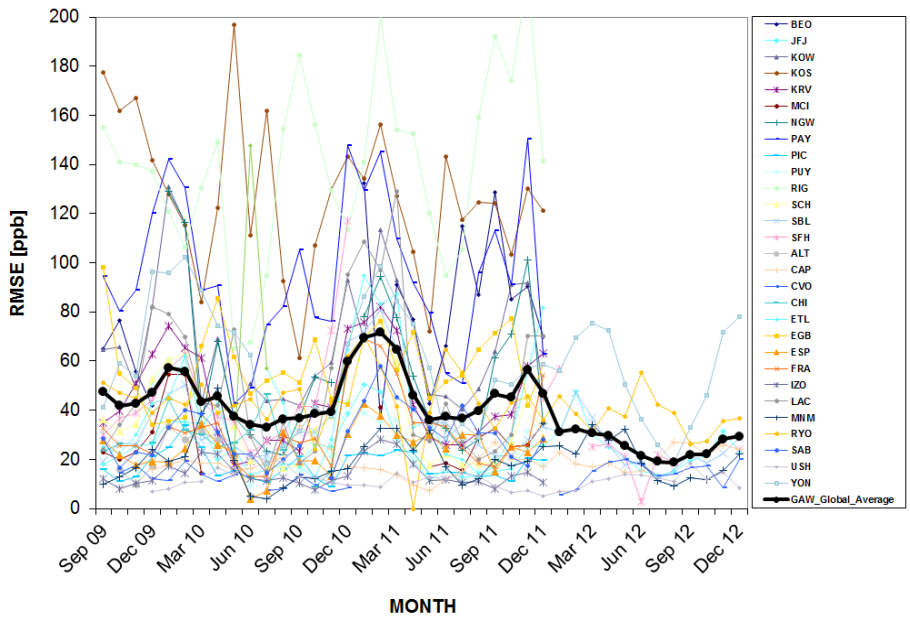
Gelöscht: ,

1

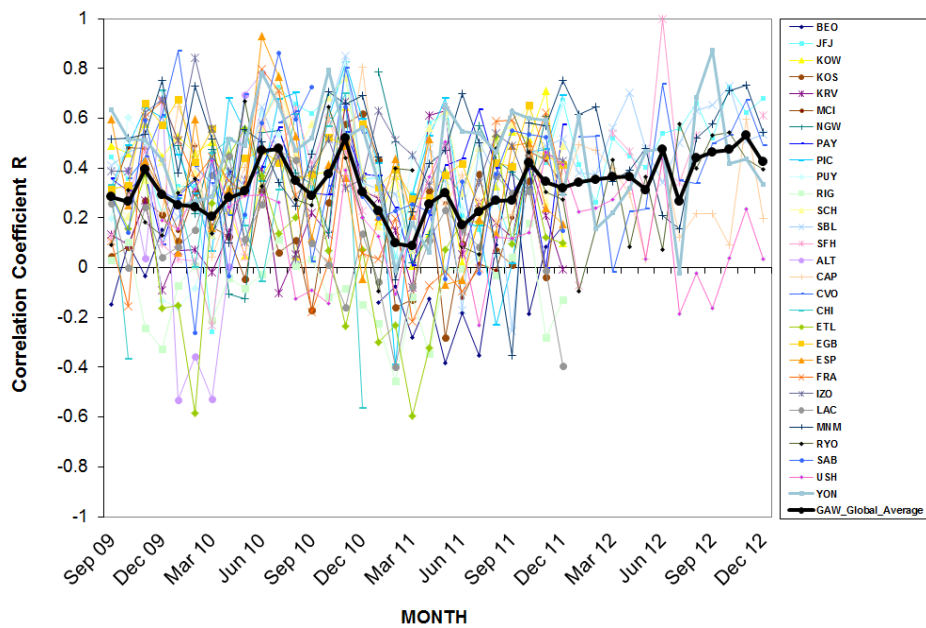


2

3 Figure 10: Modified normalized mean bias (MNMB) in % derived from the evaluation of the
4 MACC_osuite with GAW CO surface observations over the period September 2009 to
5 December 2012 (black line: global average of 29 GAW stations. Multi-coloured lines:
6 individual station results, see legend to the right).

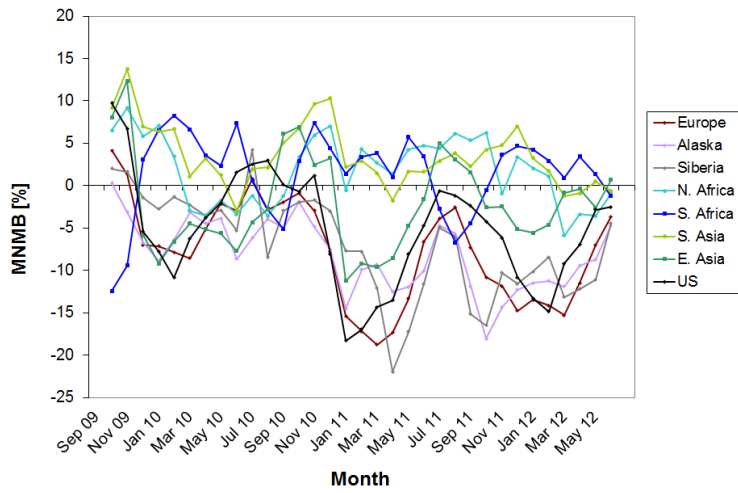


1
 2 Figure 11: Root mean square error (RMSE) in ppb derived from the evaluation of the
 3 MACC_osuite with GAW CO surface observations over the period September 2009 to
 4 December 2012 (black line: global average of 29 GAW stations multi-coloured lines:
 5 individual station results, see legend to the right).

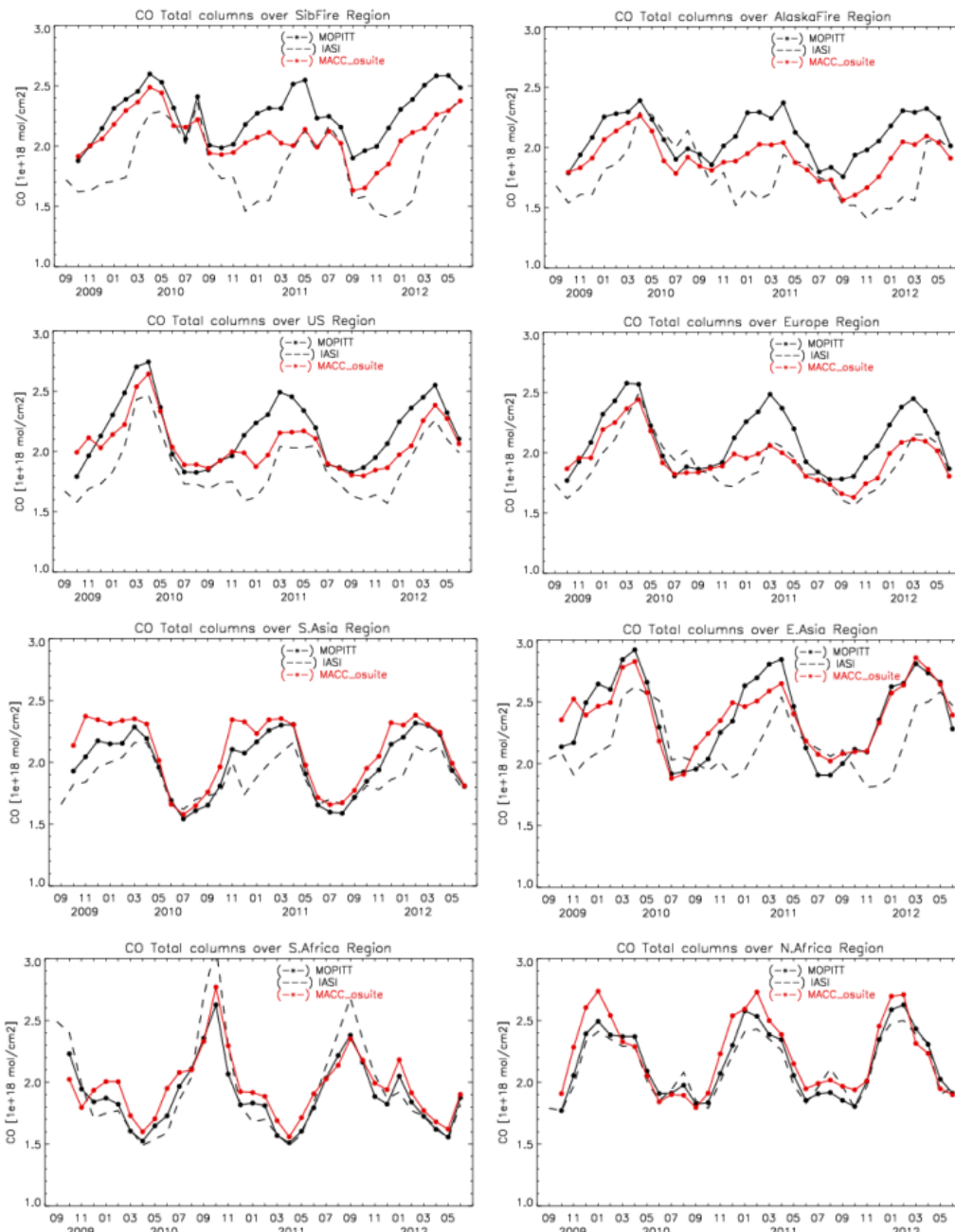


1
 2 Figure 12: Correlation coefficient (R), derived from the evaluation of the MACC_osuite with
 3 GAW CO surface observations over the period September 2009 to December 2012 (black
 4 line: global average of 29 GAW stations. Multi-coloured lines: individual station results, see
 5 legend to the right).

6



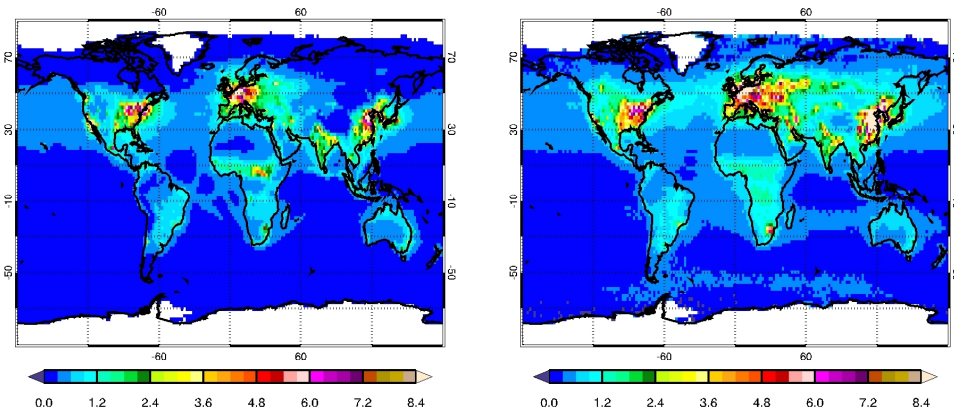
1
 2 Figure 13: Monthly average of modified normalized mean biases (MNMBs) derived from the
 3 comparison of the MACC_osuite with MOPITT CO total columns for 8 different regions
 4 during the period 09/2009 to 06/2012 (see legend on the right).



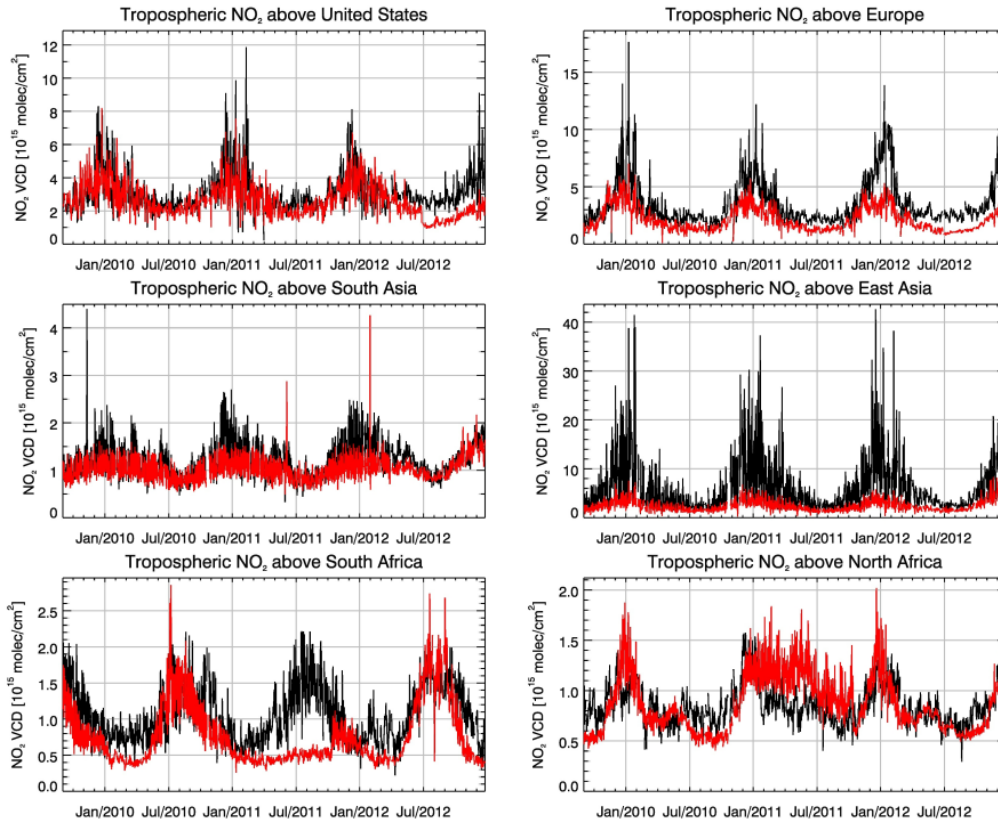
1

2

3 Figure 14: Time series plots of MOPITT CO total columns (black line) compared to IASI CO
 4 total columns (black dashed line) and the MACC_osuite CO total columns (red line) for 8
 5 different regions (defined in Figure 1) during the period 09/2009 to 06/2012. Top: Siberia
 6 (left), Alaska (right), second row: United States (left), Europe (right), third row: South Asia
 7 (left), East Asia (right) bottom: South Africa (left), North Africa (right).



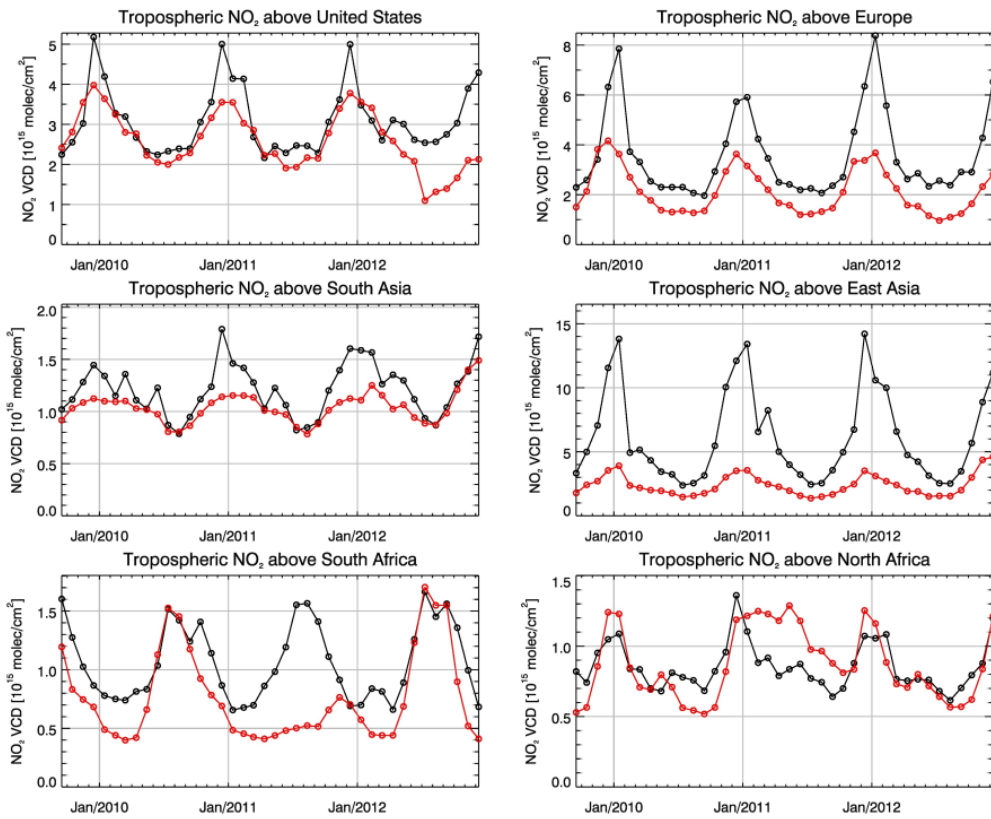
1
2 Figure 15: Long-term average of daily tropospheric NO₂ VCD [10^{15} molec cm⁻²] from
3 September 2009 to March 2012 for (left) MACC_osuite simulations and (right)
4 SCIAMACHY satellite observations. Blue colours represent low values; red/brown colours
5 represent high values.



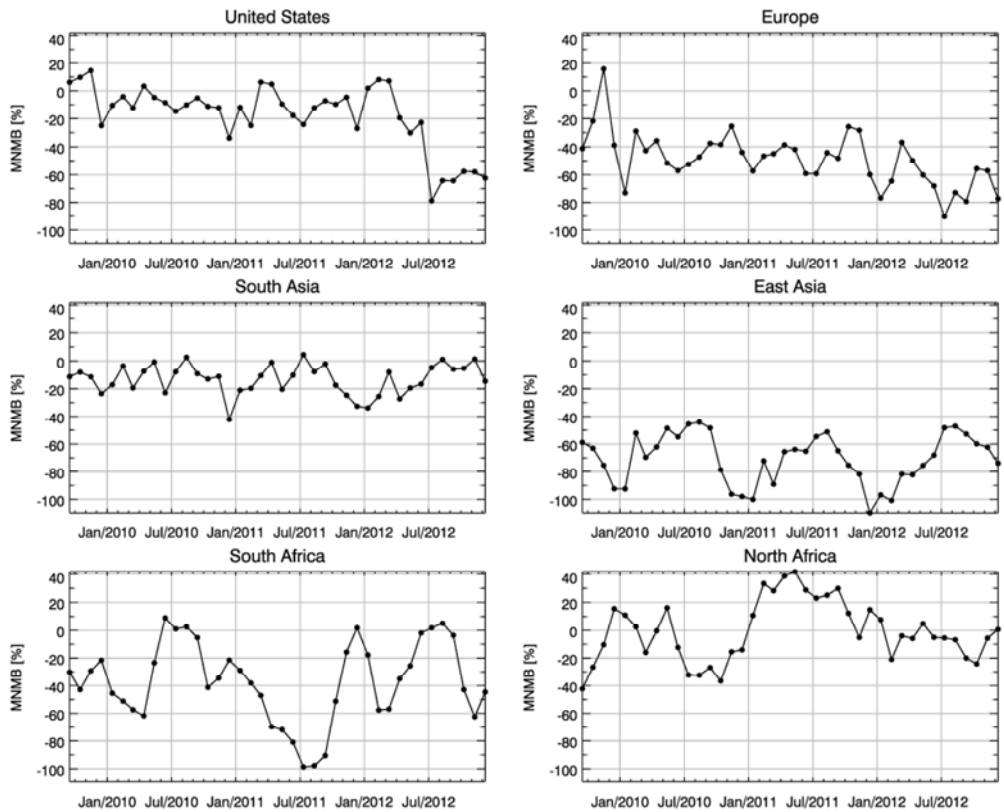
2

3 Figure 16: Time series of daily tropospheric NO₂ VCD [10¹⁵ molec cm⁻²] averaged over
 4 different regions. Top: United States (left), Europe (right), second row: South Asia (left), East
 5 Asia (right), bottom: South Africa (left), North Africa (right). Black lines show satellite
 6 observations (SCIAMACHY up to 03/2012, GOME-2 from 04/2012 to 12/2012), red lines
 7 correspond to the MACC_ouite simulations.

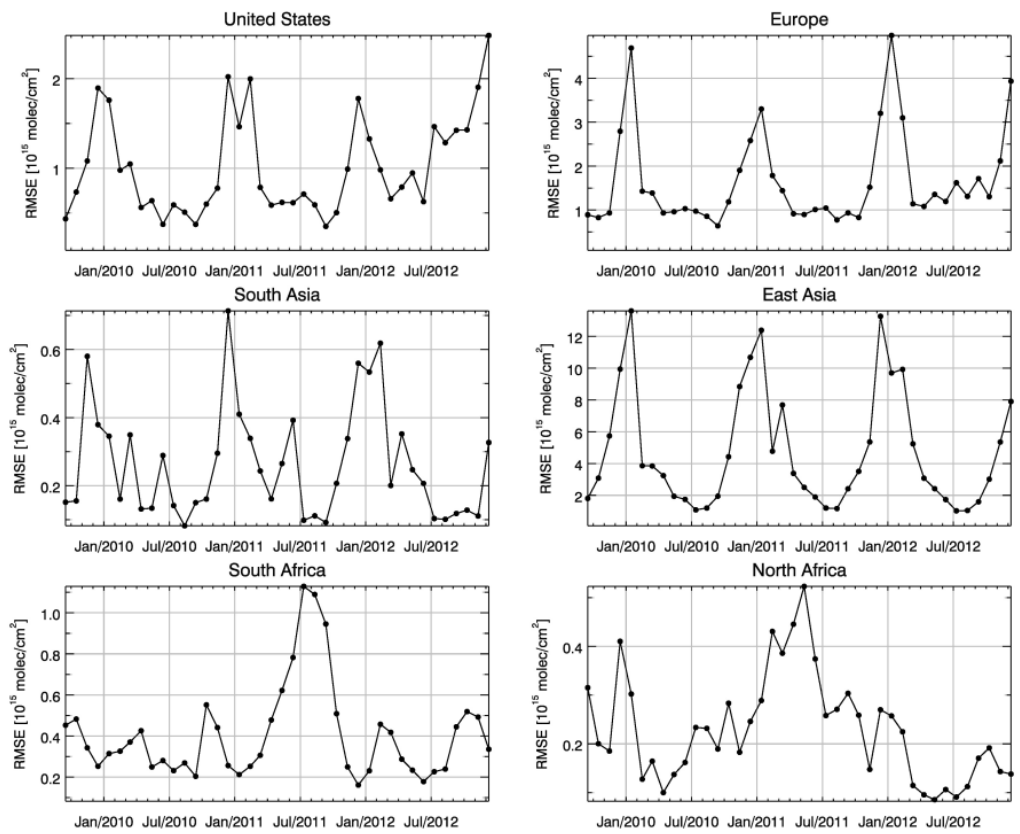
8



1
 2 Figure 17: As in Fig. 16 but for monthly means of daily tropospheric NO₂ VCD [10^{15} molec
 3 cm^{-2}] averaged over different regions. Top: United States (left), Europe (right), second row:
 4 South Asia (left), East Asia (right), bottom: South Africa (left), North Africa (right).

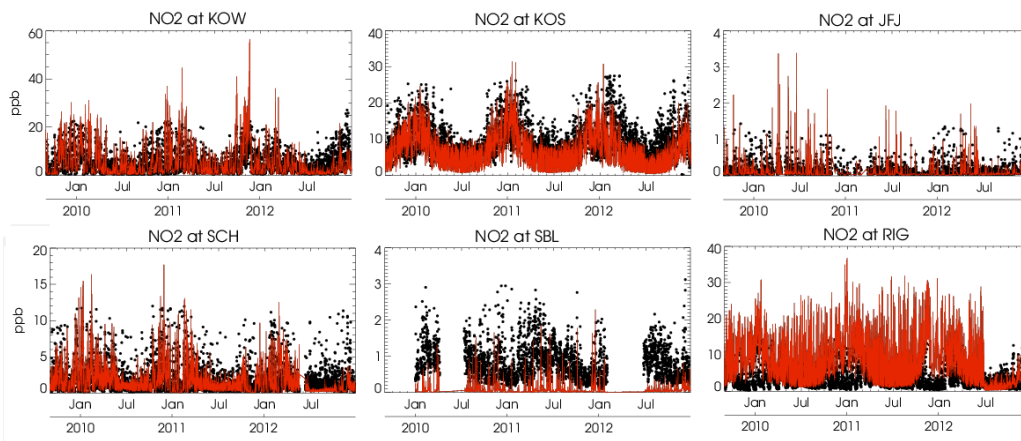


1
 2 Figure 18: Modified normalized mean bias [%] for monthly means of daily tropospheric NO₂
 3 VCD averaged over different regions (see Fig.1 for latitudinal and longitudinal boundaries)
 4 derived from the MACC_osuite simulations and satellite observations (SCIAMACHY up to
 5 03/2012, GOME-2 from 04/2012 to 12/2012). Top: United States (left), Europe (right),
 6 second row: South Asia (left), East Asia (right), bottom: South Africa (left), North Africa
 7 (right). Values have been calculated separately for each month.



1

2 Figure 19: As in Fig. 18 but for the root mean square error [10^{15} molec cm⁻²].



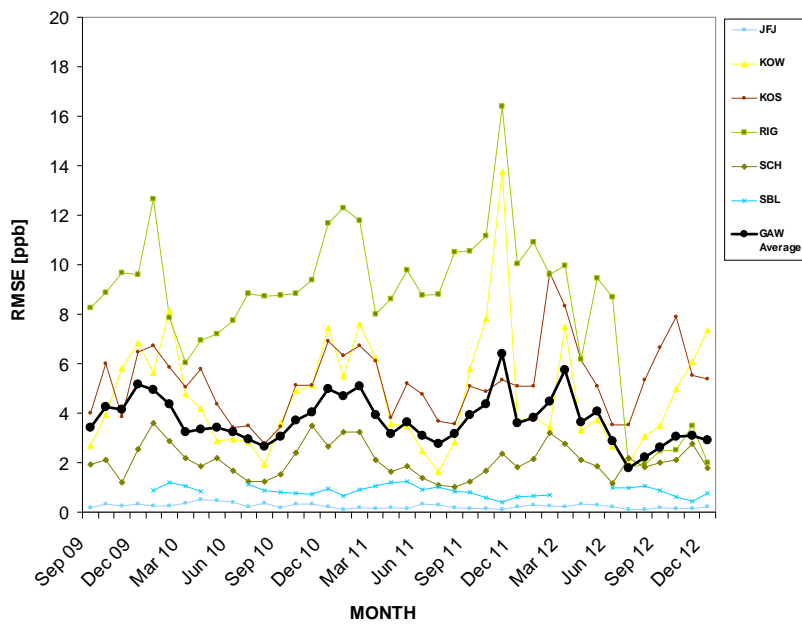
1
 2 Figure 20: Time series plots of the MACC osuite 6-hourly NO₂ mixing ratios (red) and GAW
 3 surface observations (black) for Kollumerwaard- KOW (Netherlands), Kosetice-KOS (Czech
 4 Republic), Jungfrauoch- JFJ (Switzerland), Schauinsland-SCH (Germany), Sonnblick- SBL
 5 (Austria) and Rigi-RIG (Switzerland) during the period 09/2009 to 12/2012. Unit: ppb.

Formatiert: Tiefgestellt



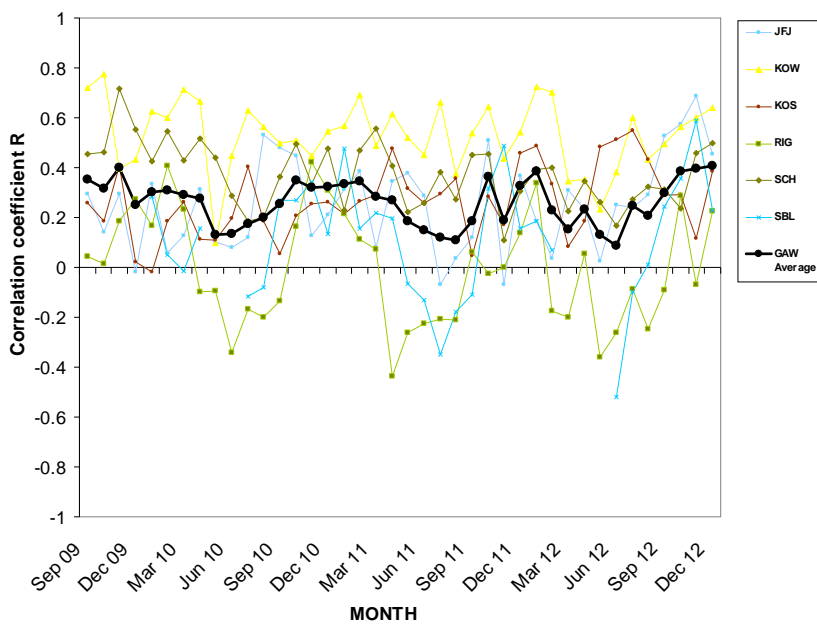
1
 2 Figure 21: Modified normalized mean bias (MNMB) in % derived from the evaluation of the
 3 MACC osuite with GAW NO₂ surface observations over the period September 2009 to
 4 December 2012 (black line: global average of 6 GAW stations. Multi-coloured lines:
 5 individual station results, see legend to the right).

Formatiert: Tiefgestellt



1
 2 Figure 22: Root mean square error (RMSE) in ppb derived from the evaluation of the
 3 MACC osuite with GAW NO₂ surface observations over the period September 2009 to
 4 December 2012 (black line: global average of 6 GAW stations multi-coloured lines:
 5 individual station results, see legend to the right).

Formatiert: Tiefgestellt



1
2
3
4
5
6

Figure 23: Correlation coefficient (R), derived from the evaluation of the MACC suite with GAW NO₂ surface observations over the period September 2009 to December 2012 (black line: global average of 6 GAW stations. Multi-coloured lines: individual station results, see legend to the right).

Formatiert: Tiefgestellt

Seite 12: [1] Formatiert

wagner

10/09/2015 16:32:00

Englisch (Großbritannien), Tiefgestellt

Seite 12: [2] Gelöscht

wagner

22/10/2015 10:43:00

is very useful to check whether there is a negative or positive deviation between model and observations. W

Seite 12: [3] Formatiert

wagner

22/10/2015 10:40:00

Englisch (Großbritannien)

Seite 12: [4] Gelöscht

wagner

22/10/2015 10:46:00

and is robust with respect to outliers.